

DOE/PN/38195--T3

LARGE SCALE STEAM VALVE TEST

**Performance Testing Of Large Butterfly Valves And
Full Scale High Flowrate Steam Testing**

RECEIVED

JAN 16 1995

OSTI

DISCLAIMER

This report was prepared as an account of work sponsored by an agency of the United States Government. Neither the United States Government nor any agency thereof, nor any of their employees, makes any warranty, express or implied, or assumes any legal liability or responsibility for the accuracy, completeness, or usefulness of any information, apparatus, product, or process disclosed, or represents that its use would not infringe privately owned rights. Reference herein to any specific commercial product, process, or service by trade name, trademark, manufacturer, or otherwise does not necessarily constitute or imply its endorsement, recommendation, or favoring by the United States Government or any agency thereof. The views and opinions of authors expressed herein do not necessarily state or reflect those of the United States Government or any agency thereof.

MASTER

DISTRIBUTION OF THIS DOCUMENT IS UNLIMITED

file

111

LARGE SCALE STEAM VALVE TEST
PERFORMANCE TESTING OF LARGE BUTTERFLY VALVES AND
FULL SCALE HIGH FLOWRATE STEAM TESTING

By

**J. B. Meadows
G. E. Robbins
D. G. Roselius
J. R. Sears, III
B. P. Moore
C. E. Young
M. S. Kasper
J. L. Joslin
J. L. Dietvorst**

Published May 1995

**Work Done and Report Prepared by
NEWPORT NEWS SHIPBUILDING, Newport News, Virginia Under Subcontract to
Westinghouse Electric Corporation Under Contract 73-R-N140302-S**

Released by

WESTINGHOUSE ELECTRIC CORPORATION



Table of Contents

| <u>Description</u> | <u>Page</u> |
|--|-------------|
| List of Figures | iii |
| List of Tables | iv |
| 1. Abstract | 1 |
| 2. Executive Summary | 3 |
| 3. Introduction | 5 |
| 3.1 Purpose of the Testing Program | 5 |
| 3.2 Scope of Report | 7 |
| Initial Steam Testing | 7 |
| Redesign | 7 |
| Scale Model Testing | 7 |
| Large Scale Steam Valve Testing Program | 7 |
| 3.3 Historical Background | 9 |
| 3.3.1 Initial Steam Testing | 9 |
| Extrapolation Technique | 9 |
| 3.3.2 Major Concerns | 10 |
| 3.3.3 Valve Redesign | 11 |
| 4. Preliminary Scale Model Testing | 15 |
| 4.1 Liquid Entrainment Concerns | 15 |
| 4.2 Comparison of Old and New Discs | 17 |
| 4.2.1 Air-Shut Valve Geometry | 17 |
| 4.2.2 Computational Methods and Analysis | 19 |
| NASA Studies | 19 |
| General Dynamics Studies | 20 |
| 2-D Vs. 3-D Effects | 23 |
| 4.2.3 Disc Differential Pressure Stress Analysis | 28 |
| 4.3 Scale Model Testing | 29 |
| 4.3.1 Test Facility Description | 29 |

Table of Contents (Cont'd)

| <u>Description</u> | <u>Page</u> |
|---|-------------|
| 4.3.2 Extrapolated Torque Values Based on Test Data | 31 |
| 5. The Need for Full Scale Testing | 33 |
| 6. ETEC Facility Design and Instrumentation | 35 |
| 6.1 Steam Supply Facility Description | 35 |
| 6.2 Test Facility Instrumentation | 39 |
| 6.2.1 Pressure | 39 |
| Static Pressure | 39 |
| Differential Pressure | 39 |
| 6.2.2 Temperature | 39 |
| 6.2.3 Piping Flowrates | 39 |
| 6.2.4 Valve Instrumentation | 39 |
| Shaft Torque | 39 |
| Disc Position | 40 |
| Actuator Differential Pressure | 40 |
| Seal Inflation Pressure | 40 |
| 6.2.5 Steam and Water Source Facility Instrumentation | 40 |
| 6.3 Data Acquisition | 41 |
| 7. Steam Flow Testing | 43 |
| 7.1 Valve Closing Tests | 43 |
| 7.2 Full Open Disc Torque, Measured Vs. Predicted | 47 |
| 7.2.1 Dry Steam Flow | 47 |
| 7.2.2 Wet Steam Flow | 50 |
| 8. Summary and Conclusions | 57 |
| 9. References | 59 |

List of Figures

| | <u>Description</u> | <u>Page</u> |
|--------------|--|-------------|
| Figure 3.3-1 | Old Valve Disc Flow Pattern | 12 |
| Figure 3.3-2 | New Valve Arrangement | 14 |
| Figure 4.2-1 | New Valve Disc Flow Pattern | 18 |
| Figure 4.2-2 | Old Disc Versus New Disc Flow Areas | 18 |
| Figure 4.2-3 | Mach Numbers on Old Valve Disc, Results of NASA Studies | 21 |
| Figure 4.2-4 | Mach Numbers on New Valve Disc, Results of NASA Studies | 22 |
| Figure 4.2-5 | Old Valve Disc Pressure Distribution, Results of General Dynamics Studies | 24 |
| Figure 4.2-6 | Old Valve Disc Velocity Distribution, Results of General Dynamics Studies | 25 |
| Figure 4.2-7 | New Valve Disc Pressure Distribution, Results of General Dynamics Studies | 26 |
| Figure 4.2-8 | New Valve Disc Velocity Distribution, Results of General Dynamics Studies | 27 |
| Figure 4.3-1 | Scale Model Valve Disc Steam Test Facility | 30 |
| Figure 6.1-1 | ETEC Facility Steam and Feedwater System Diagram | 36 |
| Figure 7.1-1 | Valve 2 Closing Test, Dry Steam, 100% Quality (Test 8) | 44 |
| Figure 7.1-2 | Valve 2 Closing Test, 28% Quality Steam (Test 13) | 45 |
| Figure 7.2-1 | Comparison of Measured and Predicted Valve Flow-Induced Torques in Dry Steam (Test 17) | 48 |
| Figure 7.2-2 | Comparison of Measured and Predicted Valve Flow-Induced Torques in Wet Steam (Test 46) | 51 |
| Figure 7.2-3 | Comparison of Valve Torques to Related Parameters (Test 45) | 53 |
| Figure 7.2-4 | Comparison of Valve Torques to Related Parameters (Test 46) | 54 |

List of Tables

| | <u>Description</u> | <u>Page</u> |
|-------------|--|--------------------|
| Table 4.2-1 | Old and New Valve Flow Areas | 19 |
| Table 4.3-1 | Full Scale Extrapolated Flow-Induced Torques | 32 |

1. **Abstract**

This report presents the results of the design testing of large (36-inch diameter) butterfly valves under high flow conditions. The two butterfly valves were pneumatically operated air-open, air-shut valves (termed valves 1 and 2). These butterfly valves were redesigned to improve their ability to function under high flow conditions. Concern was raised regarding the ability of the butterfly valves to function as required with high flow-induced torque imposed on the valve discs during high steam flow conditions. High flow testing was required to address the flow-induced torque concerns. The valve testing was done using a heavily instrumented piping system. This test program was called the Large Scale Steam Valve Test (LSSVT). The LSSVT program demonstrated that the redesigned valves operated satisfactorily under high flow conditions.

2. Executive Summary

The purpose of this report is to document the testing of large butterfly valves used in a steam piping system. These valves are pneumatically operated air-open, air-shut valves (termed valves 1 and 2). The main emphasis is placed on the results of the Large Scale Steam Valve Test (LSSVT), which tested the butterfly valves with high flow conditions from October 1989 to May 1990.

Three extensive test reports, references 1 through 3, regarding flow-induced torque on butterfly valves in high flowrates raised concerns about the ability of the valves to function as required under high flowrates. To address these concerns initial flow testing was performed in late 1987. However the test facility was capable of providing only dry steam flow at a peak flowrate of 1 million lbm/hr. These capabilities were still significantly lower than required flowrates and were transient. The following parameters were measured during these tests for use in extrapolating to flow-induced torques at higher flowrates: flow-induced torque, mass flowrate, and pressure. The extrapolated torques resulting from this testing exceeded the capability of the existing valves.

The valve was therefore redesigned to enable it to better function under high flow conditions. Redesign efforts concentrated on reducing the torque generated by high velocity flow over the full open valve disc and ensuring parts subjected to high torque are structurally adequate.

It was concluded that two aspects of the existing disc design contributed to high torque—its thickness and non-symmetrical shape. The thickness was reduced over much of the disc cross-section by replacing the continuous valve shaft with a split shaft, opening up more available flow area through the valve, which would reduce local flow velocity, and thereby, reduce torque. The disc symmetry was greatly improved by providing a curvature to the bottom half of the disc that is nearly equal to that of the top half. The old disc had a flat bottom and a pronounced upper surface curvature. The new disc symmetry results in more similar pressure distributions on the top and bottom of the disc, tending to cancel much of the resultant aerodynamic force on the disc, thereby reducing torque. Computational analyses of the redesigned valve disc indicated a significant reduction in torque.

Experimental verification of the torque reduction was then pursued via scale model testing of both the old and new valve discs. The tests indicated that the new valve disc offered a torque reduction of 52% over the old disc. The data also provided for extrapolation to a full scale flow-induced torque based on the new disc shape.

In order to fully demonstrate the capabilities of the valve, it was decided that full scale, high flow testing was required to adequately address uncertainties such as scale model factors, effects of entrained liquid, and order of magnitude flowrate differences. The test piping system was heavily instrumented to measure pressures, differential pressures, temperatures, flowrates, and steam densities. The valves were instrumented to monitor all aspects of their performance. In all, approximately 340 channels of instrumentation were recorded at a typical rate of 10 to 12 samples per second.

2. (Cont'd)

A total of 84 test runs were conducted to fully test the valves. The valves were able to close against flows of about 1.4 million lbm/hr dry steam and 1.9 million lbm/hr wet steam and endured maximum flowrates of about 3 million lbm/hr dry steam and in excess of 9 million lbm/hr wet steam in the full open position.

At the maximum dry steam flowrate, the flow-induced torques on the valves were much lower than those extrapolated from the scale model tests. Several factors, which are described in detail in section 7.2.1, are cited as possible contributors to the difference between predicted and measured torques. Valve shaft bearing friction reduced the measured torque since the shaft strain gages used for measurement had to be located outside of the bearing because of space constraints. The scale model test valve used roller bearings which have much lower frictional resistance than the sleeve bushings in the full size valve, thereby allowing more flow-induced torque to be transmitted past the bearing to the strain gages. Also, analysis of the scale test data likely resulted in a conservatively high predicted torque. Since the scale model test facility was not instrumented to measure the amount of liquid condensate in the steam accumulators, any liquid present was neglected, resulting in a calculated scale test flowrate less than actual. Therefore, resulting torque extrapolations based on the scale test calculated flowrates were higher than if the liquid condensate could have been accounted for. Other remaining possible contributors to the difference between predicted and measured torques include differences in the amount of turbulence in the flow between the scale model tests and the LSSVT, tending to reduce full scale torque, as well as uncertainty in the exponent used on the diameter ratio scale factor which directly affects the torque extrapolation.

At the maximum wet steam flowrate, the measured flow-induced torques on the valves also were less than those extrapolated from the scale model tests, especially in the case of valve 1 torques. All factors contributing to the dry steam torque discrepancy also apply to the wet steam flow. In addition to these factors, the assumption that the wet steam behaves as a homogenous mixture—essentially a gas with a density equal to the wet steam mixture density at the specified quality—results in a conservatively high extrapolated torque. This is because the entrained liquid does not generate torque in proportion to its density, as does a gas.

An unexpected observation was made regarding the flow-induced torques on the valves in wet steam flow. As the flow ramped up at the beginning of a test, the upstream and downstream valve (valve 1 and valve 2, respectively) torques followed each other closely as expected. However, during each wet steam test, a point was reached where the valve 1 torque decreased and the valve 2 torque greatly increased, almost simultaneously, during the flow ramp-up so that the valve 2 torque was several times greater than the valve 1 torque. Several theories are proposed in section 7.2.2 to explain mechanisms by which entrained liquid could cause this torque divergence.

3. Introduction

This section describes the purpose of the Large Scale Steam Valve Test (LSSVT) program and summarizes the scope of the report.

3.1 Purpose of the LSSVT Program

The LSSVT program for the butterfly valves was initiated to demonstrate that the redesigned valves would operate satisfactorily under high steam flow conditions. The valves are pneumatically operated air-open, air-shut butterfly valves (termed valves 1 and 2). As initial testing evolved through scale model testing and low flow (less than 1 million lbm/hr) full scale valve testing, it became evident that high flow testing would be necessary to address the uncertainties associated with high steam flow conditions. These uncertainties included the accuracy of flowrate extrapolations on an order of magnitude scale, the accuracy of scale model factors, and the effect of liquid entrainment (low quality steam) on flow-induced torques.

3.2 Scope of Report

This report describes the background for the redesign effort, the key issues in the valve redesign and how they were addressed, and presents the results of the testing and analyses that were performed in association with the redesign of the butterfly valves. The results of the testing of the original design valves as well as scale models and full scale prototypes of the redesigned valves are included.

Initial Steam Testing

The original design valve was tested at a facility that was capable of producing dry, saturated steam at 110 psig. This steam was used to conduct full scale valve tests at a peak, though short lived, flowrate of 1 million lbm/hr. From the results of this testing, flow-induced torques under predicted high flow conditions were extrapolated from the measured torques at the lower flowrates. These extrapolated torque values pointed to the need to improve the design of the valve to reduce the flow-induced torque, upgrade the torque handling capability, and ensure operability in high flow conditions.

Redesign

NNS improved the design of the butterfly valves for high steam flow conditions. Design criteria included the need to reduce flow-induced torque and provide sufficient material strength and actuator power. Preliminary analysis was performed which revealed that a nearly symmetrical, low profile disc would decrease flow-induced torque. Two-dimensional computer flow analyses performed by NASA Langley on both the old and new discs demonstrated the improvement in the new designs. Additional studies conducted by General Dynamics further supported the advantages of the new disc configuration.

Scale Model Testing

Once the new disc design was analyzed, its reduced flow-induced torque characteristics were verified through scale model testing. Twenty-inch diameter scale model discs were tested using dry, saturated steam at an approximate flowrate of 1.5 million lbm/hr for 2 to 3 second intervals.

Large Scale Steam Valve Test (LSSVT) Program

Full scale testing of the redesigned valves was performed at the Energy Technology Engineering Center (ETEC), in Canoga Park, CA. The LSSVT program used high pressure steam accumulators to produce dry steam (100% quality) flowrates in excess of 2.76 million lbm/hr and wet steam (as low as 25% quality) flowrates in excess of 9.18 million lbm/hr. During testing, the redesigned valves and piping were all fully instrumented to record results. The instrumentation allowed for real time recording of flowrates, pressures, densities, stresses, strains, and valve torques on tape for later data reduction. The LSSVT program demonstrated that the redesigned valves were capable of functioning properly under high steam flow conditions.

3.3 Historical Background

Prior to the LSSVT program, initial tests were conducted to determine the ability of the existing valve design to operate in high steam flow conditions. This testing was in response to concerns raised in references 1 through 3 about the potentially detrimental effect of high flow-induced torques on the valve disc at high flowrates. The results from this testing were used as a basis for the redesign of the valve.

3.3.1 Initial Steam Testing

The original design valve underwent initial steam testing. The primary objective of this testing was to obtain sufficient flow and resulting valve characteristic data to determine the adequacy of the valve to withstand high steam flowrates. The test facility was capable of producing dry steam flow only (approximately 100% quality). The steam accumulators were limited to 110 psig due to control valve pressure limitations. With this limited source, only transient flowrates significantly lower than required were attainable. The peak flowrate was approximately 1 million lbm/hr which decayed after a few seconds. To derive the desired information from the testing, an extrapolation technique was needed to estimate the flow-induced torques at higher flowrates.

Extrapolation Technique

The flow-induced torques on the valve disc under high flow conditions were extrapolated from the torque data measured at the lower flowrates during initial steam testing. The extrapolation technique used was based on the assumption that flow-induced torque was generated by the aerodynamic lift on the disc. Since dynamic pressure is the only independent variable in the lift equation (for a given disc geometry and size), it was assumed that torque is directly proportional to dynamic pressure. Dropping the common terms, the equation reduced to:

$$\left(\frac{T}{\rho V^2 r_2} \right)_{PREDICTED} = \left(\frac{T}{\rho V^2 r_2} \right)_{TEST}$$
$$T_{PREDICTED} = T_{TEST} \left(\frac{\rho V^2_{PREDICTED}}{\rho V^2_{TEST}} \right)$$

3.3.1 (Cont'd)

For ease of comparison to various flow conditions, the above equation was reduced further by creating a constant, based on tested parameters, designated as the proportionality ratio (PR).

$$PR = \frac{\rho V^2_{TEST}}{T_{TEST}}$$
$$T_{PREDICTED} = \frac{\rho V^2_{PREDICTED}}{PR}$$

where $T_{PREDICTED}$ = predicted torque (ft-lbs)
 ρ = steam density (lbm/ft³)
 V = flow velocity (ft/sec)

The dynamic pressure was calculated from values measured during initial steam testing (mass flowrate and upstream pressure) assuming dry, saturated steam conditions. The dynamic pressures for the high flowrate scenarios (both wet and dry cases) were based on flowrate, pressure, and densities associated with the high flowrates. The density used for the wet steam case (which assumes 100% liquid entrainment) was based on the assumption that the low quality steam would behave as a homogeneous flow. This assumption results in a conservatively high dynamic pressure because, in actuality, the largest part of the density component (liquid phase) is not expected to behave like the gaseous phase. The conservative assumption of homogenous flow for the low quality tests was made because the behavior of the entrained liquid in the high flow regime is unknown.

3.3.2 Major Concerns

Based on the initial steam testing, and later confirmed to a great extent by scale model testing, the flow-induced torque at high wet flowrates would hinder valve operation. Speculatively including the additional mass of entrained water as a homogeneous fluid of increased flow density resulted in large extrapolated torques.

The extrapolated torques were expected to be conservatively high. This was based on the conservative assumption that the liquid contributed to the torque in proportion to its mass fraction. However, it was suspected that the entrained water in the flow may not effectively follow streamlines around the disc, minimizing its contribution to flow-induced torque. Aside from direct impingement by the entrained water, the torque on the disc was believed to be generated mostly by the dry fraction of the flow.

3.3.2 (Cont'd)

Another major concern is the ability of the disc to pass the high flow. NASA and General Dynamics 2-D computer flow simulations (see section 4.2.2) predicted the formation of a shock front in the throat formed by the high crown of the original disc design. The shock front would form at a relatively low input Mach number. In addition to restricting flow the shock front would cause a moment great enough to hinder valve operation.

To summarize, the major goals for the redesigned valve were:

- Minimum resistance to high velocity flow.
- Minimal tendency for premature local shock wave formation.
- Substantial reduction in flow-induced torque.
- Adequate strength for high flowrate conditions.

3.3.3 Valve Redesign

The valve must, with minimum restriction, absolute stability, and structural integrity, cope alternately with high velocity flow and high pressure. The following major design objectives were most influential in the redesign of the valve:

- Minimum resistance to high velocity flow.
- Minimal tendency for local shock wave formation.
- Reduction of flow-induced torque in the full open position.
- Adequate strength for high flowrate conditions.

In addition, the following considerations had significant impact on the redesign of the valve:

- Retention of at least some minimal and consistent flow-induced torque in the opening direction in the full open position, to ensure valve stability.
- Establishment of a strong, finely adjustable full open stop for the valve.
- Retention of the basic operating method and actuator design of the existing valve.
- Sufficient strength and rigidity of the actuator bracket.

3.3.3 (Cont'd)

The existing valve disc had a flat bottom, spherical crown shape, with the seal engaging the rim of the flat bottom, and a through shaft enclosed by the crown. Additional shaft support was provided by square blocks attached to the spherical surface. The flow characteristics of the original disc design imposed potential limitations on flow. Since the rim of the disc tends to act as a flow separator, and is necessarily offset towards one side of the pipe with the valve open, flow characteristics on the two sides of the disc were vastly different.

As seen in Figure 3.3-1, flow approaching the disc below the level of the rim (assuming the flat side down) was virtually unobstructed. Flow approaching above the rim, however, was impeded not only by the shaft blocks but also by the spherical portion of the disc. The crown and piping formed a venturi, accelerating flow towards a choke condition at the throat. The resulting pressure distribution caused a significant flow-induced moment, in a direction tending to open the valve beyond its nominal 90° open position.

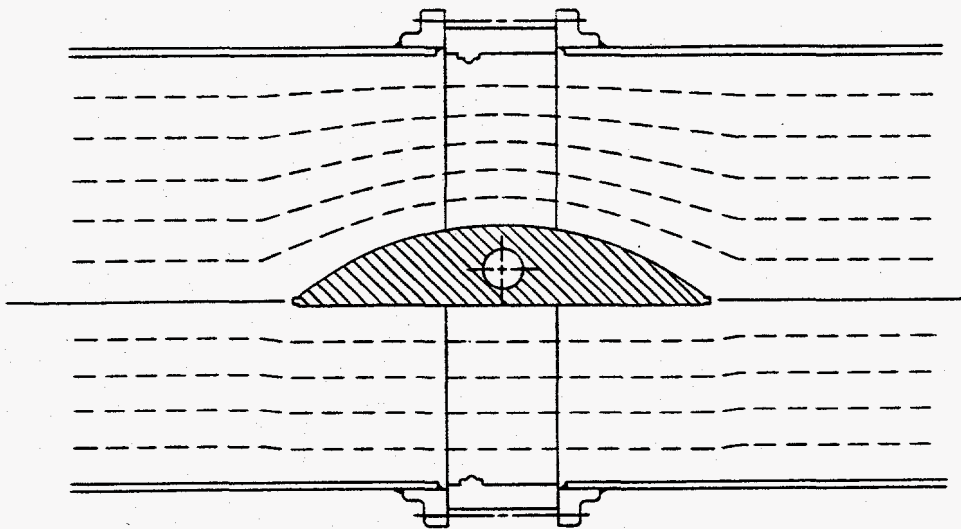


Figure 3.3-1. Old Valve Disc Flow Pattern.

3.3.3 (Cont'd)

Relief of this situation required a fundamental change to the disc configuration. The shaft, which spanned the disc and was largely responsible for the high crown shape, was separated into two stub shafts. Splitting the shaft permitted opening a flow path through the area formerly blocked by the top surface of the disc. It also permitted use of a slender, virtually symmetrical disc cross-section. The only significant deviation from the nearly symmetrical disc shape is the shaft pillow blocks, which are relatively well faired, with 45° slopes on both the upstream and downstream sides. The pillow blocks also cause a high pressure region on a portion of the upstream upper surface. This ensures stability in the open position without creating an unacceptably high flow-induced moment.

Flow characteristics of the new disc, particularly as compared to the previous disc, were extensively investigated in scale model studies (see section 4.3). Strength and flexibility characteristics were determined by three-dimensional finite element analysis using the NASTRAN computer code. Martensitic stainless steel provides a generous margin of allowable stress compared to calculated stress. Flexibility at the disc edge is within limits acceptable to the inflatable seal, as has been verified by successful testing. Finally, the weight of the new disc is nearly unchanged from the old (which was hollow), since its slender shape necessitated casting it solid.

The valve actuator bracket had to be strong enough and rigid enough to withstand possible loads imposed during the test program, without either damage or distortion.

The basic form chosen for the redesigned bracket is a closed box of steel plate, with openings as required to access bracket attachment bolts and assembly bolts. Except for minor brackets welded to suit installation of position switches and electrical boxes, the structure is symmetric about its centerline. This configuration, being a closed box, is inherently torsionally rigid. The generous enclosed area of the bracket allows the wall thickness to be held to a minimum while retaining adequate strength. The upright supporting the air cylinder pivot bracket is integrated into the basic structure. Accessories such as air control valves and electrical boxes attach directly to the smooth outer surface, with minimal need for special brackets. As a result of these features, the redesigned bracket is only slightly heavier than its predecessor, more rigid and stronger, and more easily adjustable. A valve assembly is shown in Figure 3.3-2.

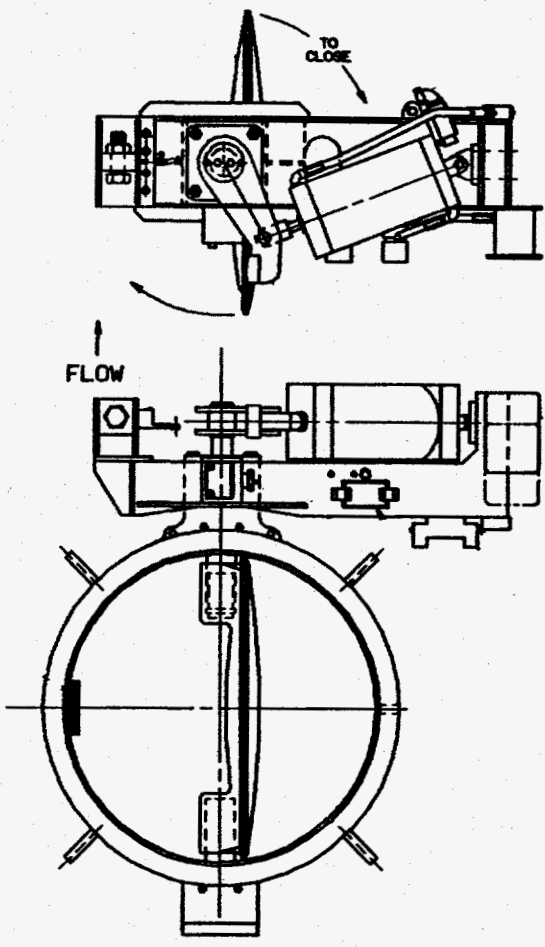


Figure 3.3-2. New Valve Arrangement.

4. Preliminary Scale Model Testing

This section discusses the redesigned valve disc, the analyses that compared flow-induced torque characteristics of the discs, and torque extrapolations to high flowrates. The section also describes preliminary scale model testing of the original and redesigned discs.

4.1 Liquid Entrainment Concerns

The presence of entrained liquid in the wet steam introduces many variables to the flow characteristics that greatly complicate pressure drop predictions. Steam at 25% quality, by definition, means that the mass of the vapor phase is 25% of the total mixture and the mass of the liquid phase is 75%. On a volume basis however, the liquid phase comprises only about 1% (at 70 psig) of the flow. The great density difference between the phases allows other parameters to affect the flow characteristics. These include droplet size, droplet size distribution, and slip ratio (defined as the ratio of vapor velocity to liquid velocity).

The problem of accurately accounting for the effects of these parameters on pressure drop is further compounded by bends and cross-sectional area transitions. At every bend the larger droplets that are unable to negotiate the turn due to their inertia are deposited on the pipe wall. This liquid is pushed along the wall by viscous forces, and it varies the otherwise predictable friction effect of a dry wall. As the liquid traverses the length of the pipe, it is repeatedly deentrained and reentrained, disturbing the flow regime and varying the effect of the mechanisms that cause pressure loss. Additional disturbances to the flow result from droplets flashing to vapor to maintain thermodynamic equilibrium as the pressure decreases throughout the pipe length, as well as from flashing and condensing of droplets due to localized pressure fluctuations.

The complexity of, and the variability in the two-phase flow regime adds uncertainty to the flowrate and pressure predictions based on the computer model, which carries over to the flow-induced torque predictions for the wet steam flow.

4.2 Comparison of Old and New Discs

The basic disc geometry, and the reasons for the changes from the old disc design to the new one, were qualitatively discussed in section 3.3. It is the intent of this section to more quantitatively discuss the design changes. This section will cover the physical comparison only; estimated performance improvement is covered in section 4.3.

4.2.1 Valve Geometry

The primary objective of this project was to reduce flow-induced torque through redesign of the valve. The best ways to lessen the flow-induced torque were to improve the symmetry of the disc and minimize the obstruction of the flow by the disc.

As discussed in section 3.3, the rim of the disc tends to act as a flow splitter, dividing the flow into a fraction which passes over the disc, and the remainder which passes under the disc. A simplified view of the original disc geometry is shown on Figure 3.3-1. This depicts, in 2-D, the condition at the piping centerline only, but is generally representative of the flow field around the old disc. Note that the rim offset from the shaft centerline channels a substantial fraction of the flow over the top surface of the disc, where it is significantly obstructed compared to the lower surface. The resulting pressure patterns create a substantial moment.

The redesigned disc is shown on Figure 4.2-1. Note that the rim offset, unchanged from before, directs the flow to a radically altered distribution of remaining open flow area. The resulting pressure fields are more nearly symmetrical, leading to a substantial reduction in flow-induced torque as discussed in detail in section 4.2.2. The pillow blocks supporting the shafts obviously affect flow, but, even including the visible portions of shaft, they directly affect less than half of the open flow diameter, defined by the T-seat retaining rings.

Figure 4.2-2 compares the open versus obstructed flow areas, in the full open position, for the new disc to those of the old disc. As is apparent in the figure, and in Table 4.2-1, the new disc maintains a more balanced relationship between the areas of the incoming flow and the areas blocked by the disc. This improvement exists both at nominal and maximum tolerance dimensions. The old disc, due to its somewhat complex hollow construction, tended to be cast on the thick side, and has been observed to be as much as 5/8 inch over nominal (minimum) thickness on the upper (curved) surface. The new disc, except for the pillow blocks, is toleranced plus/minus from nominal, and over a narrower range.

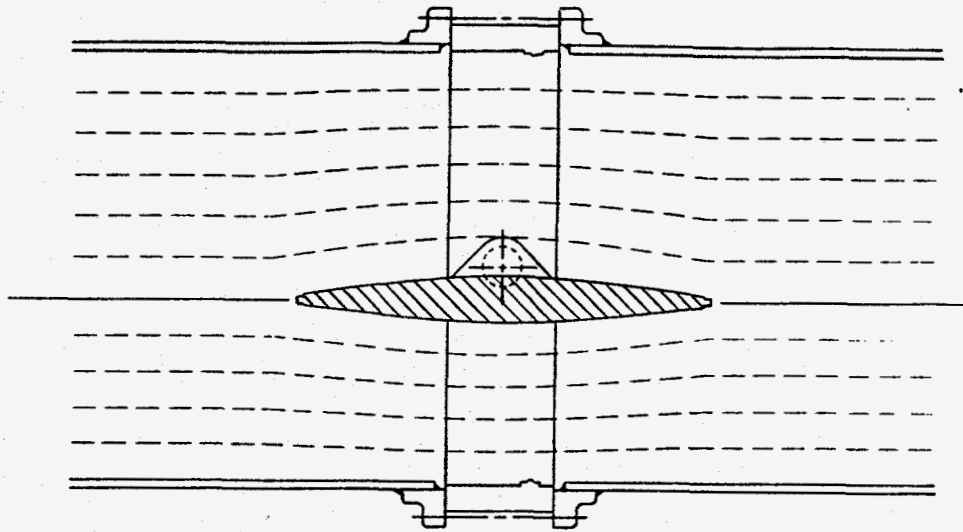


Figure 4.2-1. New Valve Disc Flow Pattern.

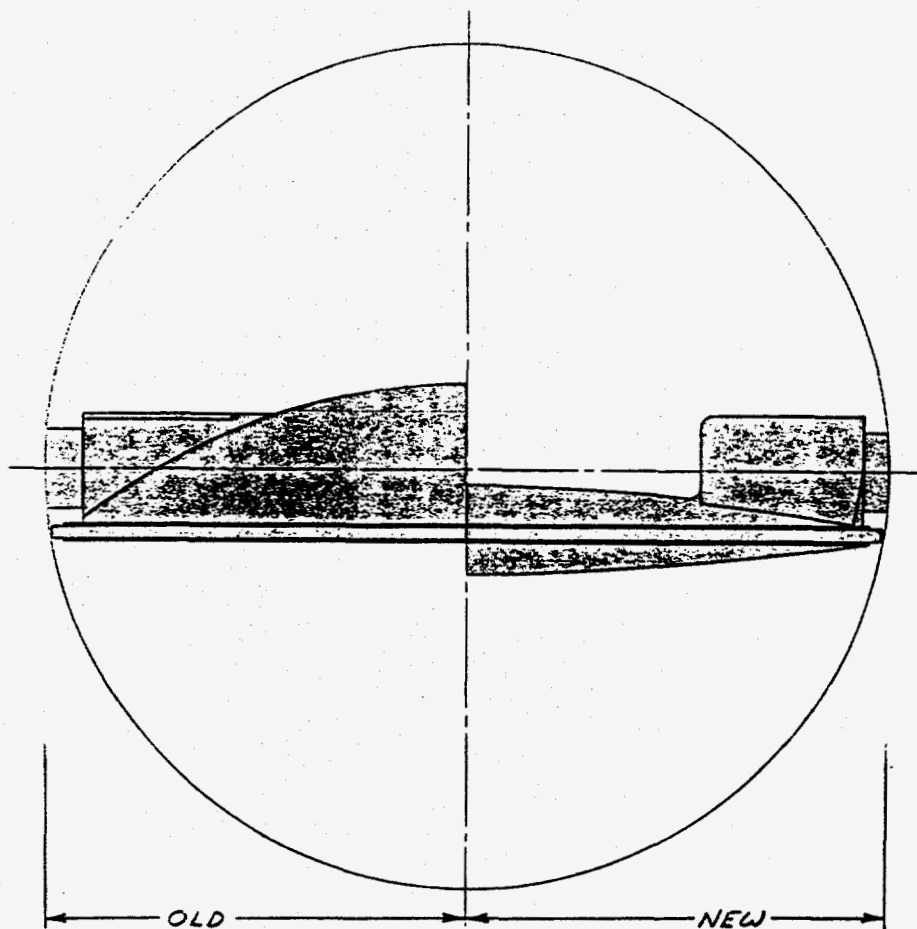


Figure 4.2-2. Old Disc Versus New Disc Flow Areas.

4.2.1 (Cont'd)

The resulting variation is both smaller and better distributed.

| PIPING FLOW AREAS ABOVE AND BELOW DISC CENTERLINE | | AREAS BLOCKED AT NOMINAL DIMENSIONS | | | | AREAS BLOCKED AT MAXIMUM TOLERANCE | | | |
|---|-----------------|-------------------------------------|------|-----------------|------|------------------------------------|------|-----------------|------|
| | | OLD DISC | | NEW DISC | | OLD DISC | | NEW DISC | |
| LOCATION | in ² | in ² | % | in ² | % | in ² | % | in ² | % |
| TOP | 557.6 | 177.2 | 31.8 | 106.5 | 19.1 | 189.8 | 34.0 | 112.2 | 20.1 |
| BOTTOM | 377.2 | 12.6 | 3.3 | 42.9 | 11.4 | 12.6 | 3.3 | 46.0 | 12.2 |
| TOTAL | 934.8 | 189.8 | 20.3 | 149.4 | 16.0 | 202.4 | 21.7 | 158.2 | 16.9 |

Table 4.2-1. Old and New Valve Flow Areas.

4.2.2 Computational Methods and Analysis

Attempts were made to analytically define the flow characteristics of the existing disc design at high flowrates, and compare the results to similar analyses of the new disc designs. Results were fairly successful at angles of attack near the full open position, particularly with regard to whether a disc design was operating at or near a choked condition at expected flowrates.

It was not feasible to analyze discs at angles of attack significantly away from full open because of the inability of available computational methods to handle flow separation that results at high angles of attack. As a result, no estimate was available for flow-induced torque for the proposed disc design at angles of attack anticipated to result in peak flow-induced torque. Peak flow-induced torque for the existing design was expected to occur at full open, at which angle the new disc was expected to produce minimal flow-induced torque. Therefore, no meaningful torque comparison could be carried out between the two designs using computers alone. Scale model testing was necessary (see section 4.3) to define flow-induced torque over a range of angles of attack.

NASA Studies

Preliminary computer flow analyses were carried out by NASA Langley personnel to estimate the maximum flow velocities around the disc resulting from input flow velocities. This work was exclusively two-dimensional, and concerned itself only with the disc cross-section at piping centerline. Results were acquired only at 0° angle of attack due to the inability of the program used to reliably predict flow separation at other angles of attack.

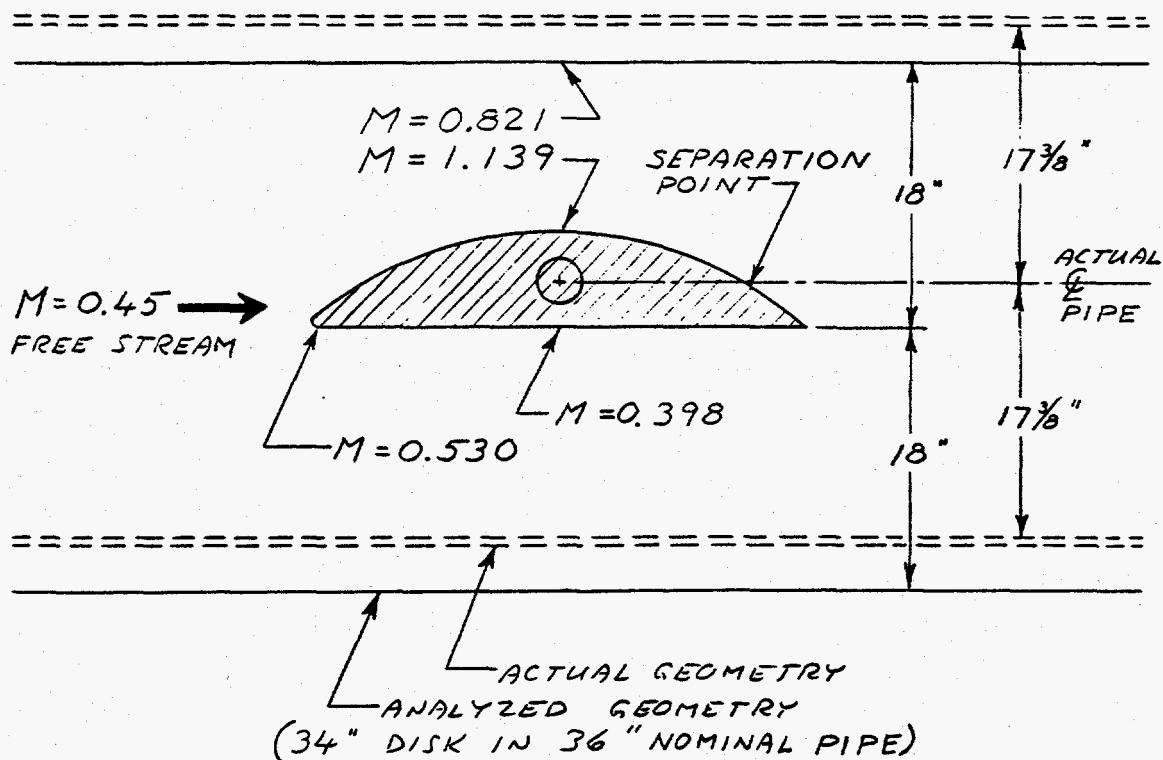
4.2.2 (Cont'd)

As shown on Figure 4.2-3, this analysis indicated that at an input Mach number of 0.45, the existing discs are expected to cause local supersonic flow near the top surface of the disc. The NASA program was developed for airfoil analysis and required minor adjustment to the disc shape, incorporating a leading edge radius. However, the analyzed shape is still representative of the existing disc. For this analysis, the bottom surface of the disc rather than the shaft axis was inadvertently centered in the pipe. The resulting shift constricted the flow above the disc more than is accurate, while opening the flow path below the disc. The error probably caused an exaggerated estimate of the Mach number over the disc. However, the error is not considered to have been very significant. The minimum flow path, as analyzed, was 64.4% as tall as the flow field captured by the disc leading edge. Shifting the pipe 3 inches, to correctly center it about the shaft axis, results in a minimum flow path representing 69.5% of the captured flow field. This is only an 8% change in constriction ratio, and would likely leave the calculated peak Mach number still supersonic. (It should be noted that the region over which the predicted Mach number exceeded 1.0 did not extend to the pipe wall. It was local to the top surface of the disc between 33% and 66% chord. Peak Mach number at the pipe wall was 0.821. While the geometry may appear similar to a converging-diverging nozzle in which flow velocity cannot exceed Mach 1 at the throat, the flow geometry is more complex than that.) The moment coefficient (defined as the moment divided by the product of dynamic pressure, area, and chord length), calculated about the quarter chord, is -0.5677. This number is primarily useful for comparison to the similarly calculated number for the new disc.

Results of the similar analysis for the new design disc are shown on Figure 4.2-4. The error on disc location did not occur in this analysis, and pipe size was set to the minimum dimension which occurs at the seal location. The only variation from the actual as built condition was a 1/16-inch shift in disc centerline offset from the shaft. The error is not considered significant, and was made in a direction which should have negligibly increased flow velocity over the disc. The throat constriction ratio, corrected, changes by 0.04%. Results of this run were very encouraging, indicating a peak Mach number of 0.614 at an input Mach number of 0.5. Flow above and below the disc was virtually the same, which resulted in a moment coefficient reduced from -0.5677 to -0.0078. The basic shape of the disc appeared virtually optimum; the object then became to disrupt it as little as possible with the addition of pillow blocks to accept the shafts. The pillow blocks were kept to a minimum size, and were positioned as near the piping walls as possible. The pillow blocks were faired into the disc with 45° slopes upstream and downstream; thus, as many of the basic flow characteristics of the disc as possible were retained.

General Dynamics Studies

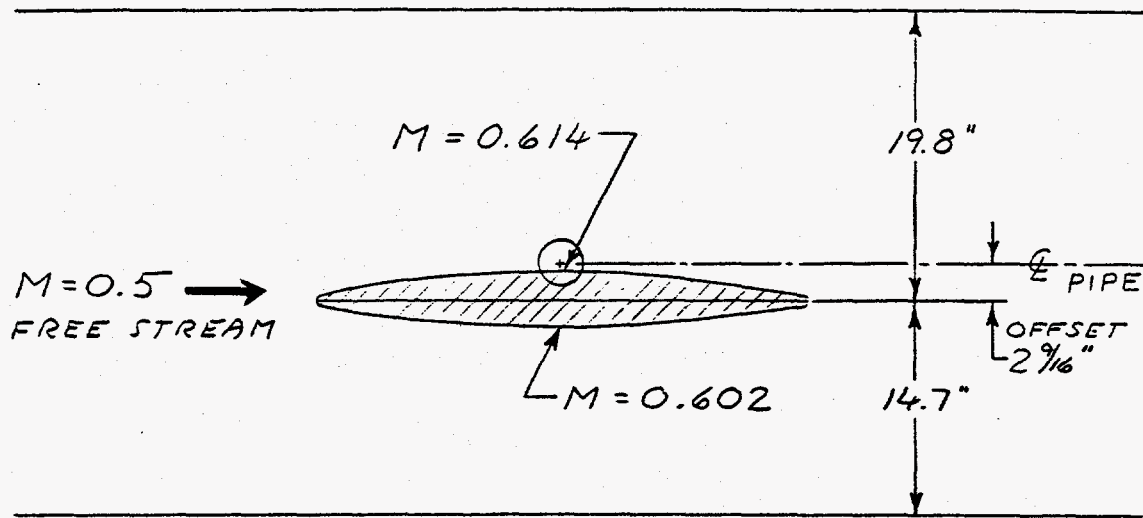
General Dynamics (GD) conducted more sophisticated studies of the existing and proposed shapes for the valve. The GD studies were similar to the NASA studies in being two-dimensional, but were more comprehensive in that they displayed, in color, both pressure and velocity fields around the discs. They also were able to explore a limited range of angles



Note: Geometry of the pipe was inadvertently centered about the disc lower surface, rather than the shaft. This led to an artificially severe constriction above the disc, slightly exaggerating the effects of disc asymmetry.

C_M at $1/4$ chord = -0.5677

Figure 4.2-3. Mach Numbers on Old Valve Disc, Results of NASA Studies.



(34" DISK IN 34 1/2" MINIMUM I.D. PIPE)

C_M at 1/4 chord = -0.0078
 No predicted separation point.

Figure 4.2-4. Mach Numbers on New Valve Disc, Results of NASA Studies.

4.2.2 (Cont'd)

of attack varying plus/minus from zero. Results generally were similar to the NASA results. The new disc design remains clearly subsonic, with very little pressure or velocity gradient surrounding it. The existing design exhibited a radical velocity gradient in the throat created by the disc crown and the pipe, and pressure fields which would clearly result in a substantial moment. Examples of the pressure and velocity fields surrounding the old and new valve designs are shown on Figures 4.2-5 through 4.2-8. In interpreting these figures, it is noted that the originals were in color, with color scales unique to each plot. For purposes of black and white reproduction, the color zones have been outlined and a numerical sequence assigned to represent all distinguishable colors. The range represented by the color scale was annotated on the computer output, and is included here correlated to the appropriate number.

The figures reproduced in this report are for an inlet Mach number of 0.37. Peak Mach number for the new disc is 0.474, distributed over a wide area of both the upper and lower surface. This contrasts with the old disc peak Mach number of 0.784, which occurs at a very local area on the top surface, after a steep velocity gradient. Furthermore, the new disc exhibits high velocity flow over the entire disc upper and lower surface, while the old disc trails a pronounced low velocity wake from its after third upper surface.

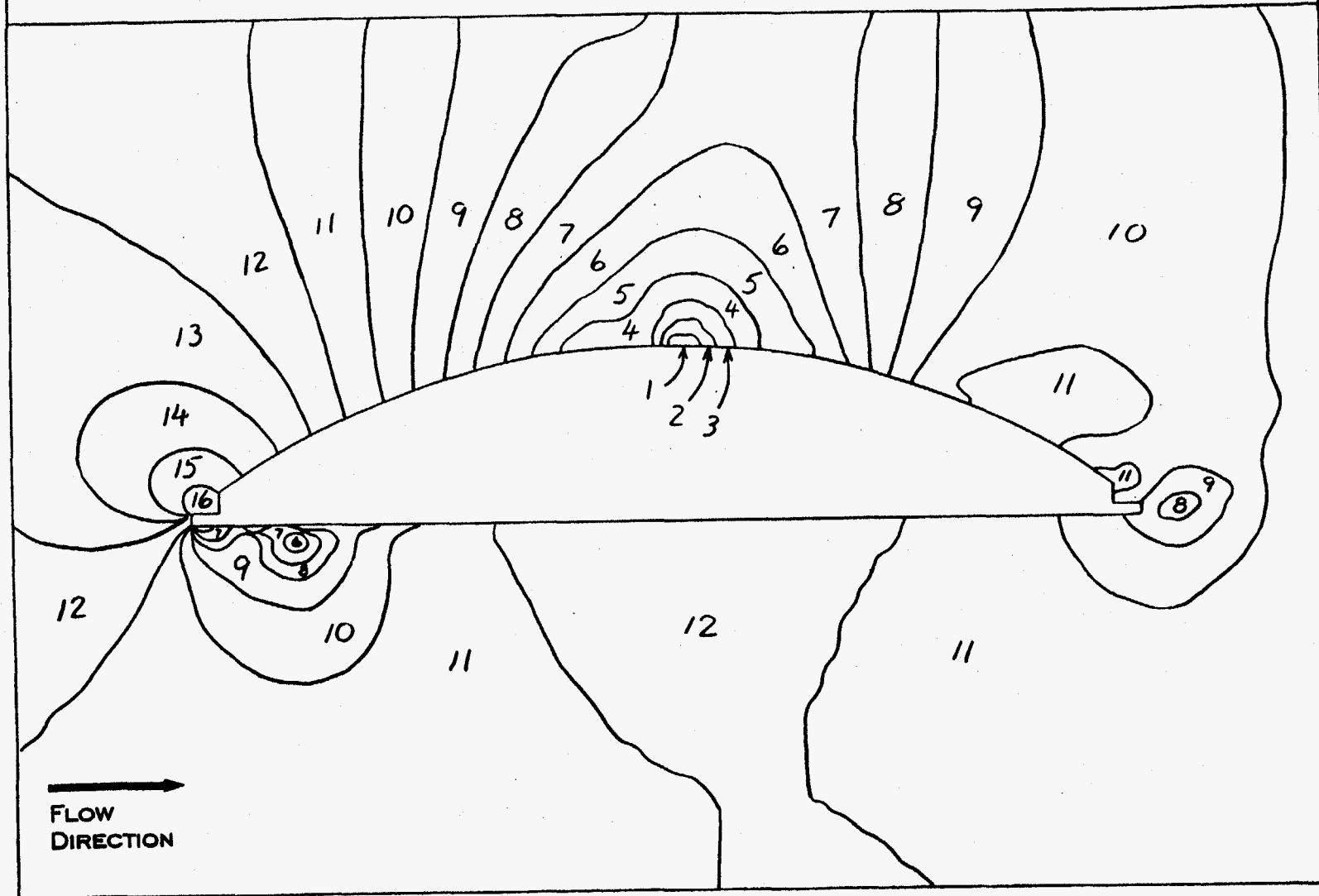
Pressure exhibits a similar contrasting behavior. The new disc is surrounded by virtually symmetrical pressure fields, unlikely to generate significant moment. The old disc, particularly in its forward quarter, exhibits high pressure on the upper surface opposite low pressure on the lower surface, leading to substantial flow-induced moment. Also, the pressure range represented by the contours on the old disc pressure plot (Figure 4.2-5) is nearly twice the range represented on the plot for the new disc (Figure 4.2-7). The rapidly increasing pressure field on the downstream upper surface of the old disc is probably largely responsible for the extensive low velocity wake. Overall, the new disc offers a substantial improvement in flow characteristics.

2-D Vs. 3-D Effects

All of the analyses conducted by NASA and General Dynamics were for 2-D flow. The disc cross-section represented was that at disc/pipe centerline, and no attempt was made to represent either the round pipe or the spanwise variation in disc cross-section. Early inquiries into the possibility of 3-D analysis were discouraging, involving several months of modeling and expensive computer runs. It was decided to use the 2-D analyses for development of basic disc geometry, followed by scale model and full scale testing. Schedule requirements dictated that construction of full size valves take place simultaneously with scale model testing.

Three-dimensional effects not accounted for in the 2-D analyses are attributable to two main sources—the pipe is circular, not rectangular, and the disc does not have a constant spanwise cross-section.

Pressure Distribution
Original Disc Geometry
Mach No. = 0.37

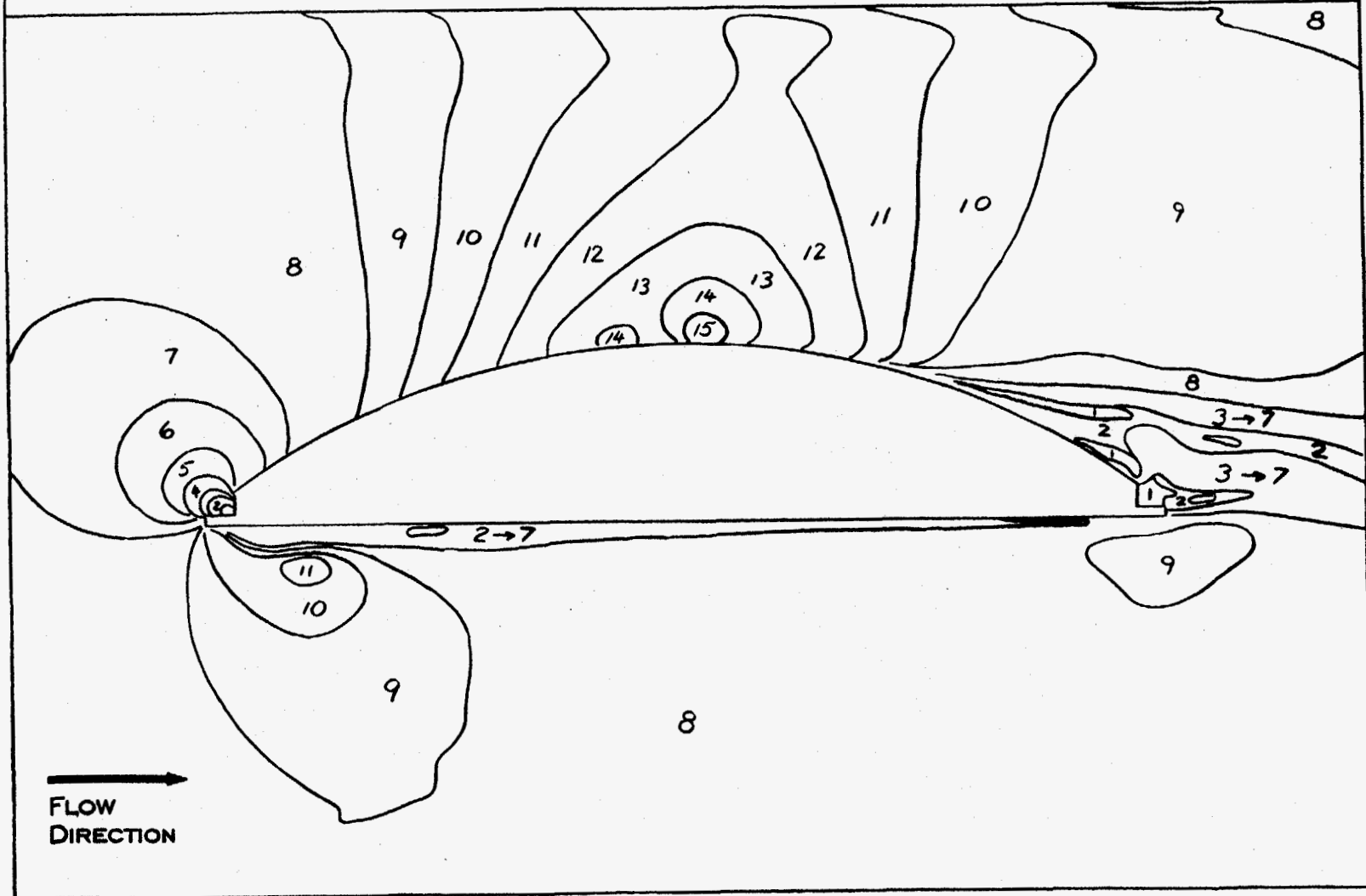


* Pressure Range:
Minimum = 0.6159 = "1"
Maximum = 1.0 = "16"

* Contours normalized to maximum pressure on disc

Figure 4.2-5. Old Valve Disc Pressure Distribution, Results of General Dynamics Studies.

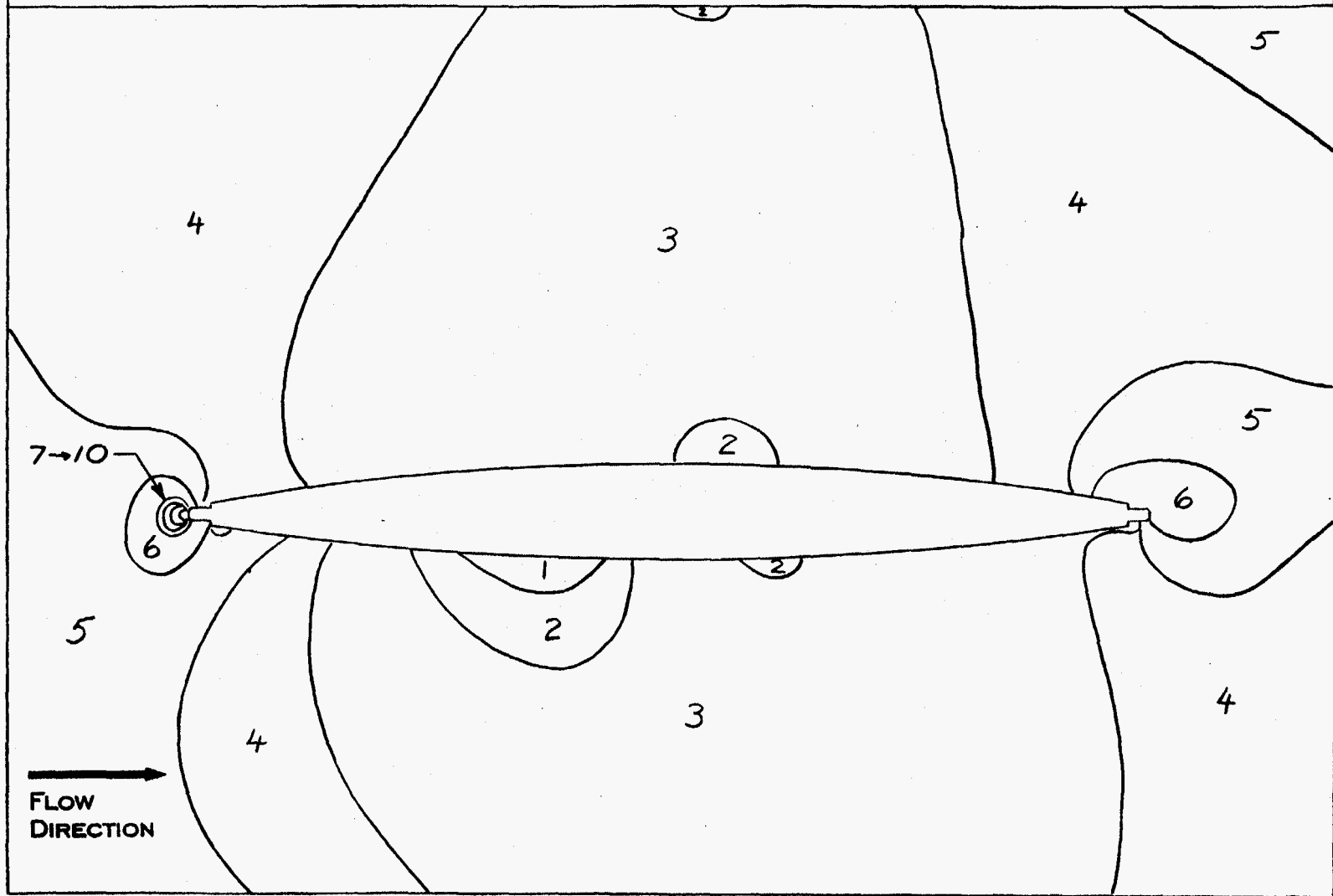
Velocity Distribution
Original Disc Geometry
Mach No. = 0.37



Mach No. Range:
Minimum = 0.0000 = "1"
Maximum = 0.7844 = "15"

Figure 4.2-6. Old Valve Disc Velocity Distribution, Results of General Dynamics Studies.

Pressure Distribution
New Disc Geometry
Mach No. = 0.37

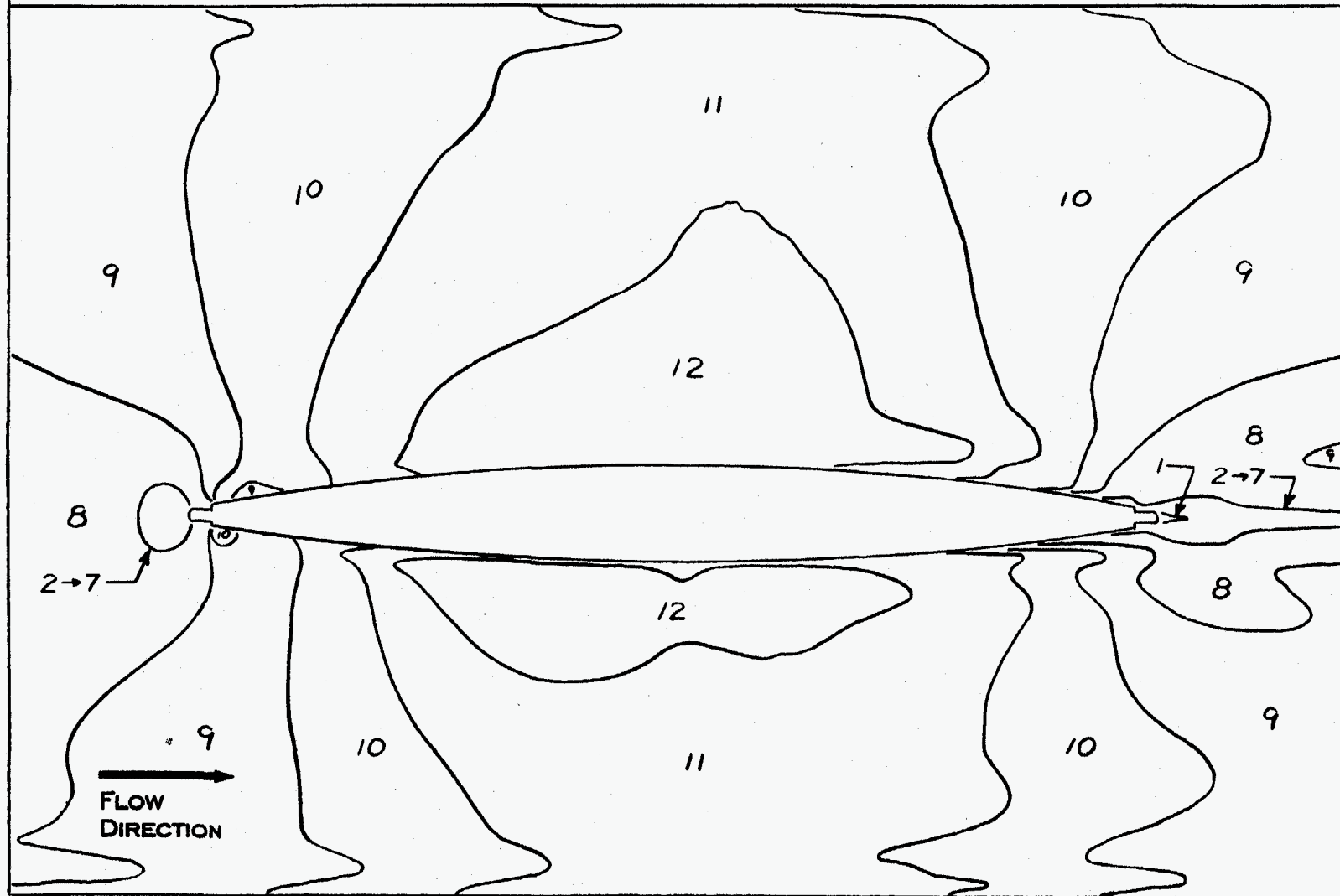


* Pressure Range:
Minimum = 0.8062 = "1"
Maximum = 1.0 = "10"

* Contours normalized to maximum pressure on disc

Figure 4.2-7. New Valve Disc Pressure Distribution, Results of General Dynamics Studies.

Velocity Distribution
New Disc Geometry
Mach No. = 0.37



Mach No. Range:
Minimum = 0.0000 = "1"
Maximum = 0.4740 = "12"

Figure 4.2-8. New Valve Disc Velocity Distribution, Results of General Dynamics Studies.

4.2.2 (Cont'd)

An effect of the non-circular pipe is that, nearer the side of the pipe, the available flow area above and below the disc decreases, resulting in locally higher flow velocity as well as a span-wise velocity component. The high pressure field upstream of the pillow blocks not present in the 2-D analysis contributes to disc moment, and the spanwise flow into the slot between the pillow blocks increases velocity over the trailing upper surface, further contributing to moment. Flow over the smooth lower surface is subject to virtually none of these effects, except possibly some spillage around the disc edge near the shafts. The most effective way to account for all these effects is flow testing. For this project dry steam flow testing was carried out at approximately 60% of full size, as described in section 4.3, to verify the reduction in flow-induced torque for the new design disc prior to the full scale test program.

4.2.3 Disc Differential Pressure Stress Analysis

Since a primary goal of the redesign effort was to improve valve flow characteristics the disc configuration was changed as previously discussed. Formerly a 6-1/2-inch thick hollow casting with internal reinforcement and a through shaft, the disc was revised to a 3-3/4-inch thick solid casting with half shafts socketed into pillow blocks. In the interest of unrestricted flow, the pillow block wall thickness was held to a minimum, necessitating finite element analyses of the disc at the high pressure differential.

Several cases on four different finite element models were run to investigate disc, shaft, and spline stresses under a variety of pressure and torsional loads. System pressure loads the upstream (smooth) face of the disc, and leak test pressure in the volume between the two valves loads the downstream (pillow block) face of the disc on the upstream valve (valve 1). Therefore it was necessary to run the pressure cases both ways. Disc and shaft stresses were virtually the same except for sign, but stress distribution local to the shaft socket in the pillow blocks was completely different and required further investigation. Also, the maximum projected torsional load was applied to a pillow block. A realistic load for the new design being unavailable pending full scale testing, the load used was extrapolated from previous testing of a similar valve disc.

Results of the computer analyses were evaluated for comparison against the disc and shaft material strengths, and to verify that disc rim deflection under pressure was consistent with the capability of the disc rim seal to deflect with the rim while maintaining a seal. The analysis results showed that the valve has generous strength margins in all components and that the maximum displacement of the disc rim will maintain a seal.

4.3 Scale Model Testing

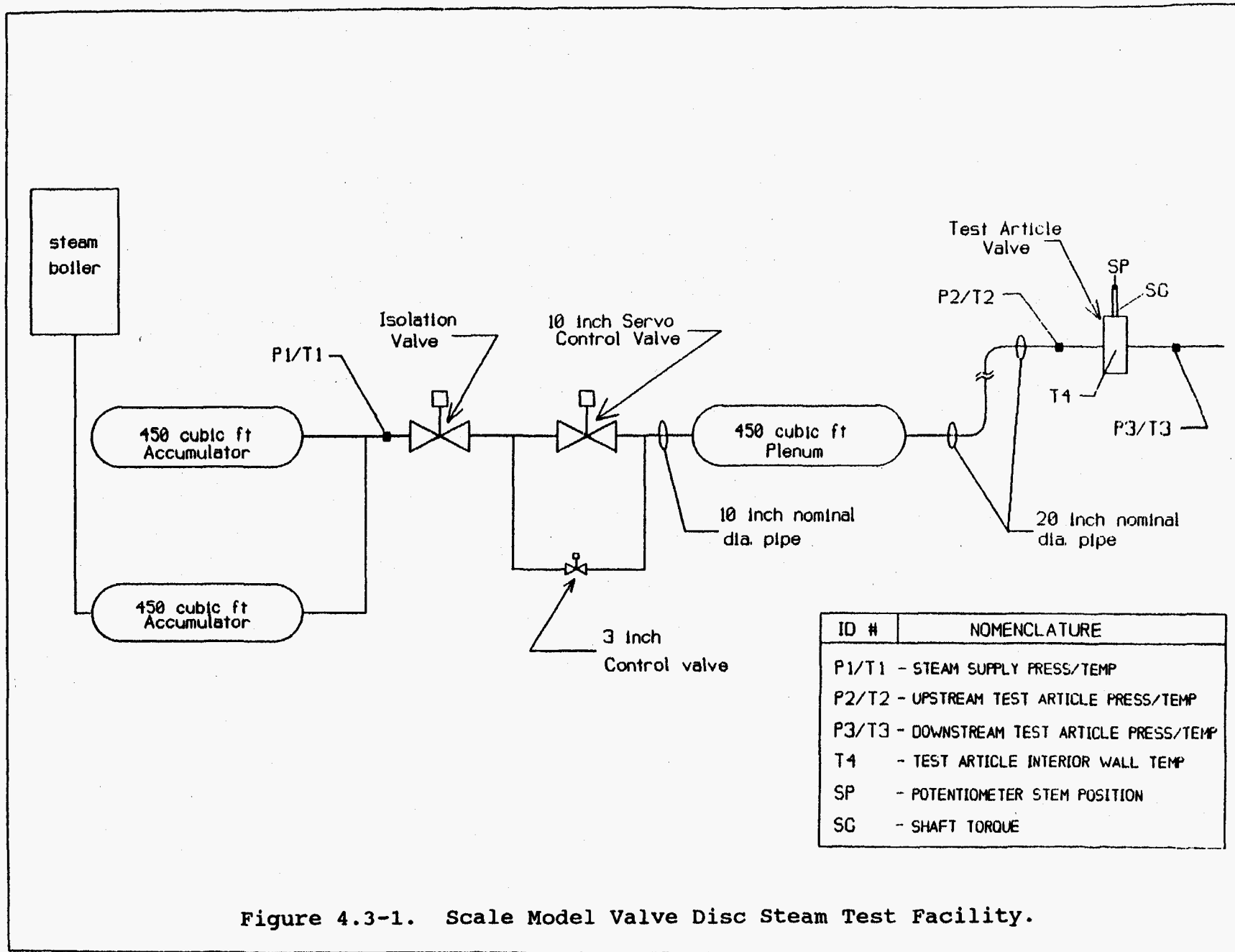
Scale model valve testing was conducted to verify improvement in disc shape based on flow-induced torque characteristics under high steam flow conditions. The best disc shape was determined to be the disc which produced the lowest magnitude of flow-induced torque with the disc in the full open position. New design disc shapes, developed independently by NNS and General Dynamics, including the original valve disc were tested.

4.3.1 Test Facility Description

The steam test facility for scale model testing consisted of a series of control valves, 20-inch nominal diameter piping, pressure and temperature taps, large volume accumulator tanks and a steam boiler (Figure 4.3-1). The steam boiler supplied dry, saturated steam to two 450 cubic foot dry steam accumulator tanks. These accumulator tanks were used to provide steam supply to the test article valve. Steam flow through the test article valve was controlled by a 10-inch servo-controlled butterfly valve and a 3-inch bypass control valve. This configuration proved capable of providing dry, saturated steam at approximately 1.5 million lbm/hr for a duration of several seconds to the test article valve.

Steam mass flowrate through the test valve was determined from the change in mass in the accumulators during each blowdown assuming that a negligible amount of liquid was initially present in the accumulators. The change in density (and therefore mass) was calculated based on recorded accumulator pressure (P1 on Figure 4.3-1), assuming dry saturated steam, over a known time interval. This method of flow measurement, though not as accurate as a flow metering device such as a venturi nozzle, was selected due to schedule and cost constraints, and because it would result in conservatively high torque predictions. The predictions would be conservative because the calculated scale test flowrate used for the extrapolation would be less than the flowrate that generates the scale test measured torque due to some of the neglected liquid flashing to vapor, adding to the flow.

Test article upstream pressure, measured approximately 5 feet upstream of test valve (P2 on Figure 4.3-1), was used to regulate the steam flowrate for each blowdown. Prior to each blowdown, a test valve upstream pressure was determined and the 10-inch control valve was remotely adjusted throughout the blowdown run to maintain this upstream pressure for a minimum of 5 seconds. Changing this pressure in approximately 10 psi increments produced a wide range of flowrates for each test valve disc position. Test article downstream pressure and temperature, measured approximately 3 feet downstream of the test article valve (P3 and T3 on Figure 4.3-1) were also recorded and used to identify any abnormalities, discontinuities or choked flow conditions produced by the test valve disc position.



| ID # | NOMENCLATURE |
|-------|--------------------------------------|
| P1/T1 | - STEAM SUPPLY PRESS/TEMP |
| P2/T2 | - UPSTREAM TEST ARTICLE PRESS/TEMP |
| P3/T3 | - DOWNSTREAM TEST ARTICLE PRESS/TEMP |
| T4 | - TEST ARTICLE INTERIOR WALL TEMP |
| SP | - POTENTIOMETER STEM POSITION |
| SC | - SHAFT TORQUE |

4.3.1 (Cont'd)

Other test valve instrumentation included a thermocouple on the valve body interior wall (T4 on Figure 4.3-1) used to verify steam conditions (saturated), a potentiometer (SP on Figure 4.3-1) located on the valve shaft used for valve disc position indication, and a strain gage bridge (SG on Figure 4.3-1) mounted on the valve shaft used to measure and record flow-induced torque on the test valve shaft. Hewlett-Packard X-Y plotters simultaneously plotted accumulator pressure, upstream test valve pressure and test valve shaft torque. This data was then available for analysis immediately following each blowdown.

4.3.2 Extrapolated Torque Values Based on Scale Test Data

Previous valve flow testing provided a basis for estimating flow-induced torque for the original valve discs. The disc shapes were redesigned to minimize flow-induced torque. Scale models of both the old and new valve discs were tested to verify the reduction in torque of the new discs. The scale model testing determined the relationship between valve torque and dynamic pressure for dry steam flow for each disc geometry at different disc angles of rotation ranging from 90° (full open) to 5° from closed in increments of 5° to 10°. Also, a neutral (zero torque) position was determined by additional tests at intermediate positions. The dynamic pressure ($\frac{1}{2}\rho V^2$) immediately upstream of the test valve was calculated using values of density and velocity, which were determined as follows. The density was taken as that for dry saturated steam at the measured upstream static pressure. The flow velocity was calculated using the mass flowrate, density, and flow area.

The scale model test data were used to estimate the full scale torques for each disc shape at high flowrate conditions. The following equation estimates full scale torque at high flowrate conditions using scale model test data.

$$T_{fs} = T_m \left(\frac{D_{fs}}{D_m} \right)^3 \frac{(\rho V^2)_{fs}}{(\rho V^2)_m}$$

where, T = Torque

D = Valve disc diameter

Subscripts _{fs} and _m denote full scale and scale model values, respectively.

The diameter ratio cubed term in this equation represents the scale factor. The validity of the scale factor exponent was evaluated by EG&G Idaho, Inc. and reported in reference 2 which studied butterfly valve torque characteristics and extrapolations of test data to much larger size valves. The EG&G tests were conducted with asymmetrical valve discs (flat on one side, curved on the other) and are therefore similar to the old valve disc, but not the new, nearly symmetrical disc. EG&G found that for closing the curved face of the disc

4.3.2 (Cont'd)

into the flow with upstream pressures from 15 to 60 psig, the diameter ratio exponent was generally below 3. Therefore, using an exponent of 3 when extrapolating to a larger valve would yield a conservatively high predicted torque. For a similar evaluation with the flat face of the disc closing into the flow, the extrapolation exponent was frequently slightly above 3, which would result in a non-conservative torque extrapolation using an exponent of 3. It is not clear which of these cases more closely represents the new design valve disc because although both faces are curved, the curvature is much flatter than the curved face of the EG&G test discs because the discs are thinner (in proportion to diameter). However, it is theorized that the primary influence is the shape of the downstream surface and how it affects the flow separation near the disc edge. It was concluded that an extrapolation exponent of 3 is reasonable considering conservatism in the high flow conditions used and the fact that the diameter ratio for the scale model tests is only 1.74 (compared to 3.0 used for the above described EG&G evaluations), which reduces the effect of the exponent.

Torque extrapolations for full open, full scale valves were made for two selected high flowrate steam conditions: 100% steam quality ("dry" steam) at an upstream dynamic pressure of 1600 psf and 23% steam quality ("wet" steam) at a dynamic pressure of 4340 psf. The extrapolation equation incorporates a linear relationship between valve torque and steam dynamic pressure. The two-phase wet steam flow was assumed to be homogenous when calculating density and velocity for simplicity and because it yields a conservative torque prediction.

Results of the full open valve torque extrapolations are listed in Table 4.3-1. It is seen that the new valve disc offers a torque reduction of about 50% from the original design. Extrapolated wet steam torques were expected to be conservatively high because the largest part of the density component (liquid phase) is not expected to follow streamlines around the disc, because of their inertia, thus minimizing its contribution to flow-induced torque. In actuality, the torque on the disc is expected to be generated mostly by the dry fraction (gaseous phase) of the flow.

| DISC TYPE | EXTRAPOLATED TORQUE VALUES (ft-lbs) | |
|-----------|-------------------------------------|-----------|
| | DRY STEAM | WET STEAM |
| OLD VALVE | 9260 | 25,200 |
| NEW VALVE | 4400 | 12,000 |

Table 4.3-1. Full Scale Extrapolated Flow-Induced Torques.

5. The Need For Full Scale Testing

As discussed in previous sections of this report, tests were conducted to evaluate the adequacy of the valves. However, there were several uncertainties that could not be resolved by the scaled or low flowrate test data, such as:

- Scale model factors
- Effects of entrained liquid
- Order of magnitude flowrate differences

In order to demonstrate the structural and functional capabilities of the valves, it was decided that full scale flow testing was required.

6. ETEC Facility Design and Instrumentation

This section describes significant features of the steam supply facility, instrumentation, and data acquisition system.

6.1 Steam Supply Facility Description

The steam and water source at ETEC included:

- A propane fired boiler (4.9×10^6 BTU/hr)
- A boiler feedwater system
- Two steam accumulator tanks (31,300 gallons each)
- One steam-water accumulator tank (38,400 gallons)
- Control valve manifold which delivered the steam-water mixture to the test piping

A simplified diagram of the steam and water facility is shown in Figure 6.1-1.

Deionized water was pumped from the feedwater system storage tank, T-3 (8,000 gallons), with pump P-3 (50 gpm) to the water supply tank, T-315 (4,000 gallons), under 25 psig nitrogen cover gas pressure. The steam/water accumulator, T-449, and the two steam accumulators, T-313 and T-314, were initially purged with nitrogen and filled with water from the water supply tank. The accumulators were heated to test pressure (maximum of 450 psig) by continuous recirculation of water through the accumulators and through the boiler, H-1, where steam was generated and injected into each vessel. Makeup water was pumped from the water supply tank with pump P-2 (50 gpm) to each accumulator hot water recirculation line where makeup water was mixed and heated during the filling process. The temperature of the recirculation water returning to the accumulators was maintained within 150 F of the accumulator water temperature. Each accumulator was equipped with a relief valve set at 500 psig; an automatic steam vent valve; crossover lines to allow pressure equalization between vessels; and instruments that monitored temperature, pressure, and water level.

Prior to steam blowdown, the upstream piping was preheated by opening bypass valve V-1212. After preheating, the piping was pressurized to accumulator pressure by opening the block valves (V-1201, V-1202, and V-1203). After preheat and pressurization, the system was turned over to the computer for initiation and control of test flow.

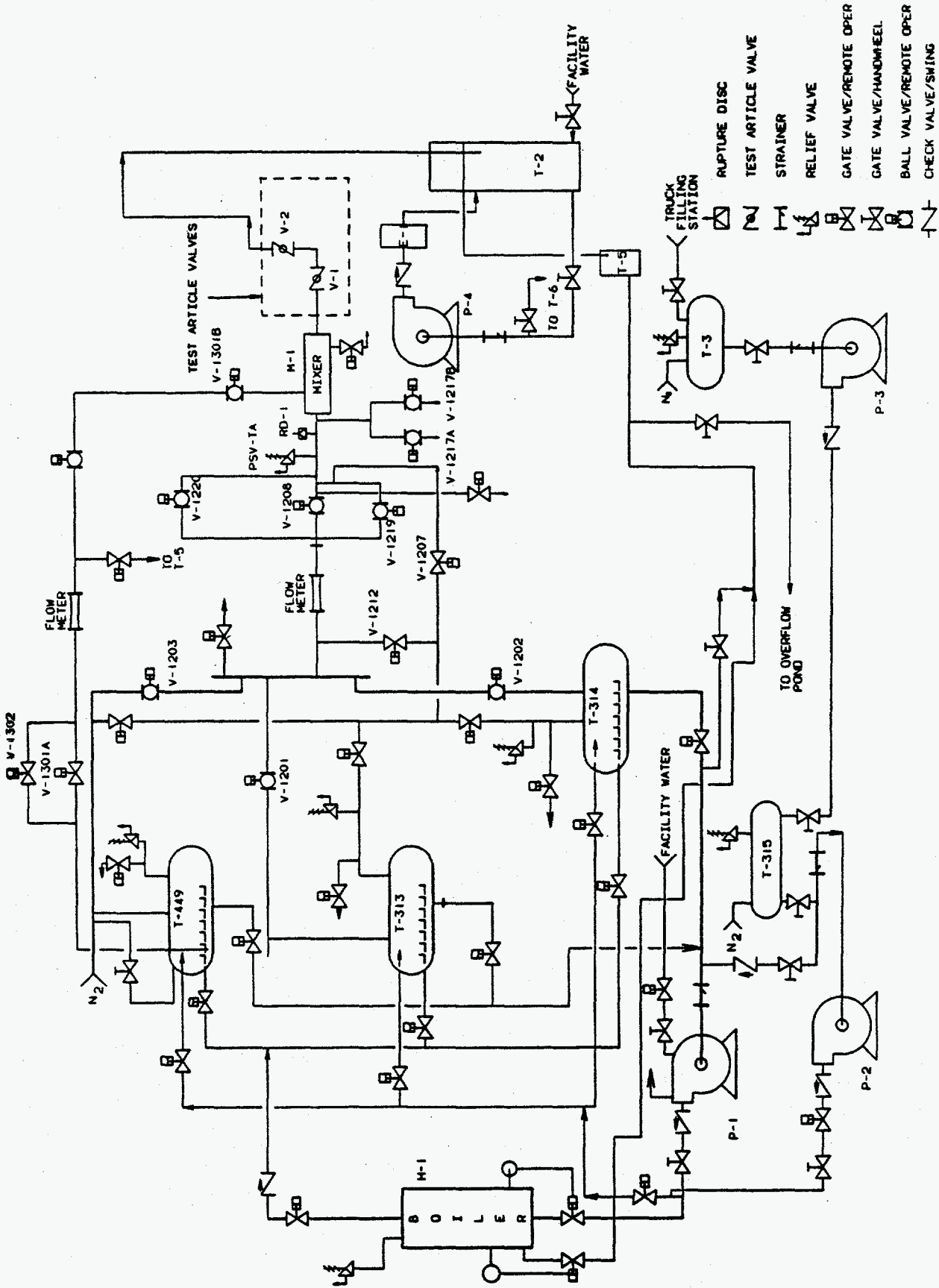


Figure 6.1-1. ETEC Facility Steam and Feedwater System Diagram.

6.1 (Cont'd)

For the wet steam tests, sub-cooled water was taken from T-449 to be mixed with steam from the other accumulators by opening V-1301A in lieu of V-1203. T-449 accumulator pressure was maintained during a blowdown by supplying additional nitrogen cover gas.

Relief valve PSV-TA (150 psig set point) and rupture disc RD-1 (either 150 psig or 250 psig burst pressure) provided overpressure protection just upstream of the mixer (M-1) located at the test piping inlet in addition to computer controlled vent valves V-1217A and V-1217B. The 250 psig rupture disc was required to compensate for high pressure differentials across the mixer for high flowrate tests.

A Komax static mixer (M-1) was used for mixing the steam and water supplied to the test piping. The mixer consisted of three stages of fixed, angled baffle plates (later modified to two stages because of excessive pressure drop) enclosed in a pipe (36-inch diameter by 110-inch long) and was designed to use the kinetic energy of the steam and water flow to accomplish the mixing. Steam entered the mixer axially and water entered the mixer through a side port that fed an internal annular ring. The internal baffles produced three mixing actions:

- Division and subdivision of the steam and water flow streams
- Intermingling the flow streams by stream to stream impingement
- Developing of counter-rotating vortices which back-mixed the phases.

The test piping inlet steam quality was calculated based on measurements of the flowrates, temperatures, and pressures of steam and water entering the mixer and the temperatures of the steam-water flow exiting the mixer (assuming constant enthalpy across the mixer and that the phases were at equilibrium).

All but three tests were conducted with a closed-loop flow control system. Either mass flowrate, piping inlet pressure, or steam quality was used for feedback signals depending on the test objectives. Steam flow was controlled by computer operation of three parallel hydraulically operated control valves (V-1208, V-1219, and V-1220). For wet steam tests, water flow was controlled by computer operation of flow control valve V-1301B programmed to control water flow based on initial accumulator conditions. The steam-water mixture was further controlled to the desired quality by operation of steam control valves based on steam and water temperatures and pressures measured upstream and downstream of the mixer.

Additional pressure control was provided upstream of the test piping by computer controlled addition of steam through valve V-1207 (and venting of steam through relief valves V-1217A and V-1217B in the event the pressure exceeded a specified maximum value).

6.2 Test Facility Instrumentation

Static and dynamic pressures, differential pressures, temperatures, flowrates, densities, valve shaft torques, valve disc positions, and valve actuator differential pressures were measured during the test.

6.2.1 Pressure

Static Pressure

Static pressure measurements were made usually with two transducers at each position (on opposite sides of the pipe).

Differential Pressure

Differential pressure transducers were located across the upstream valve (one in the plane of the disc and the other in the plane perpendicular to the disc).

6.2.2 Temperature

Fluid temperature measurements were made via a thermocouple at each pressure measurement location. The temperatures were measured in conjunction with pressure to verify saturation conditions or to determine the amount of superheat, which can result from blowing down steam from a high pressure accumulator.

6.2.3 Piping Flowrates

Primary mass flowrate measurements were made by venturi flowmeters in the steam and water supply lines to the test piping.

6.2.4 Valve Instrumentation

Shaft Torque

Strain gages on the valve shafts monitored shaft torque during steam flow testing. Due to the harsh steam environment and the limited space available on the shaft within the valve body, the strain gages were necessarily installed between the shaft bearing and actuator linkage outside of the body. Therefore, bearing friction torque was incorporated into the measured flow-induced torque (but not into the actuator torque). However, it is likely that the flow-induced vibration of the disc significantly dissipated the static friction in the bearings. The flow control system was programmed to sound an alarm in the event that a shaft torque in excess of 27,000 ft-lbs was measured on any test valve.

Disc Position

The position (in degrees) of each valve disc was measured with a potentiometer located at the end of the valve drive shaft.

Actuator Differential Pressure

The differential pressure across each test valve actuator piston was measured with a pressure differential transducer connected to taps at each end of the actuator cylinder.

Seal Inflation Pressure

The T-seat inflation pressure for each valve was monitored with an absolute pressure transducer.

6.2.5 Steam and Water Source Facility Instrumentation

The steam and water source facility at ETEC was instrumented to monitor all parameters necessary for operation, control, maintenance, and safety of the plant. Facility instrumentation of particular use for test evaluation were those which established the thermodynamic state of the steam in the accumulators and at the mixer steam and water inlets, and the flowmeters in the steam and water supply lines.

6.3 Data Acquisition

The ETEC data acquisition system (DAS) consisted of a Hewlett-Packard 1000 series computer with disc and magnetic tape drives, digital valve controllers, video display monitors and a system schematic display board. The DAS was used to remotely monitor and control the test facility steam conditions between steam blowdown tests, and monitor and control the test parameters during each steam blowdown test.

All measured parameters were stored on tape by the DAS through data channels connecting the sensing device to the computer. The data sample rate—the rate at which the DAS sampled each sensor—was typically 10 to 12 samples per second during a test for each of approximately 340 data channels. The sample rate was kept as high as possible to best capture any transient phenomena. During periods of system heat-up or between blowdown tests, the sample rate was much lower ranging from one sample per second to one sample per minute, which was sufficient to monitor test facility conditions.

The sample rates obtained during steam blowdowns were limited by the speed of the central computer and the method of sampling. The method of sampling considered to be the most efficient was to take a data sample from every data channel sequentially, thus collecting the same number of data points for each data channel. Repeating this process at a specified time interval produced the desired sample rate. Another method of sampling considered was to program the central computer to use higher sample rates at selected data channels during highly transient periods while maintaining a slower sample rate for less significant data parameters. (For example, it was desired to step up the sampling rate for the valve torque, position and upstream pressure during valve cycling.) However this method would require additional computer instruction execution time resulting in unacceptably slower sampling rates. Therefore, the former method of data sampling was selected.

Following the completion of each test, "quick look" data plots were printed via a Hewlett-Packard dot matrix printer from a disc that was limited to five samples per second. Test and system parameters were plotted versus time to provide prompt evaluation of the previous test. These plots provided adequate detail of flow and structural conditions existing through each test to determine the success of the test.

7. Steam Flow Testing

To test the adequacy of the redesigned butterfly valves, full scale steam valve testing was conducted at the Energy Technology Engineering Center (ETEC), a division of Rockwell International, located in Canoga Park, CA.

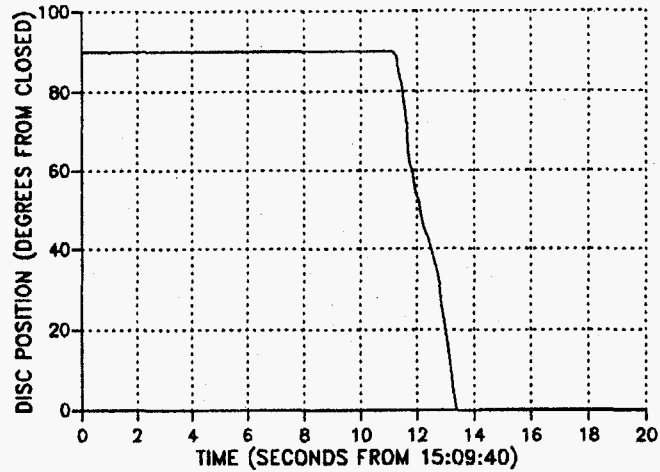
Eighty-four tests were conducted at ETEC to satisfy valve testing requirements. Deviations from the test resume occurred as the test program progressed to address specific questions and concerns generated by previous test results. Repeating tests and/or modifying the test was common to obtain information on a specific area of concern.

This section presents LSSVT results and analyses.

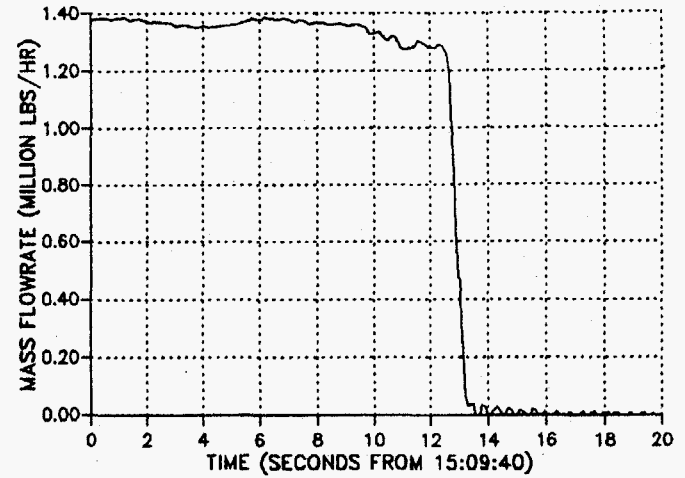
7.1 Valve Closing Tests

Testing of the valves for closing capabilities did not identify any problems with the valves. The valves were signaled to close against high flowrates (about 1.4 million lb/hr dry steam and 1.9 million lb/hr wet steam) and successfully accomplished this task. The valve torques were well within the capabilities of the valve actuator. Successful dry tests on valve 1, valve 2, and both valves closing simultaneously were conducted as Tests 7A, 8 and 9, respectively. Valve 2 had the highest resultant torque and the results of Test 8 are shown in Figure 7.1-1. The first successful wet flow test was performed on valve 2 as Test 13. The results of Test 13 were satisfactory and are shown in Figure 7.1-2.

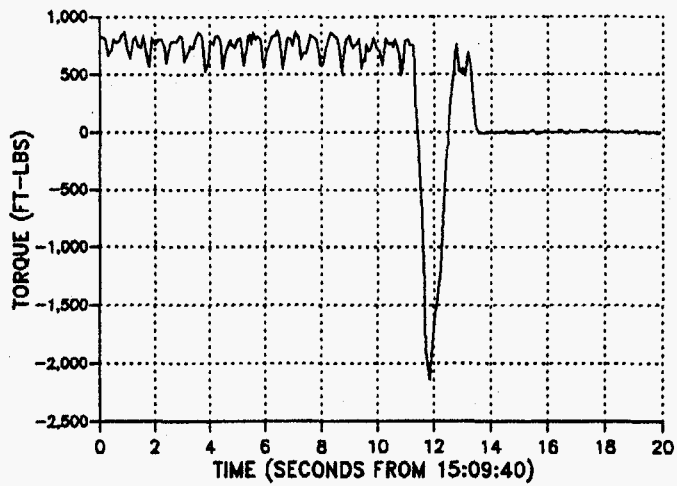
DISC POSITION



MASS FLOWRATE



VALVE TORQUE



UPSTREAM AND DOWNSTREAM PRESSURE

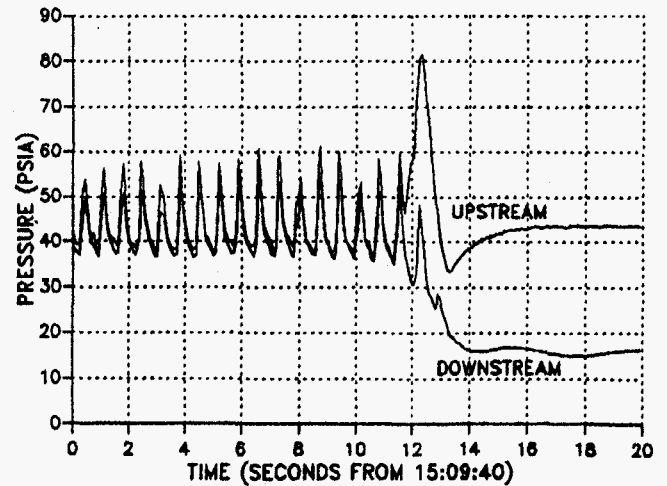
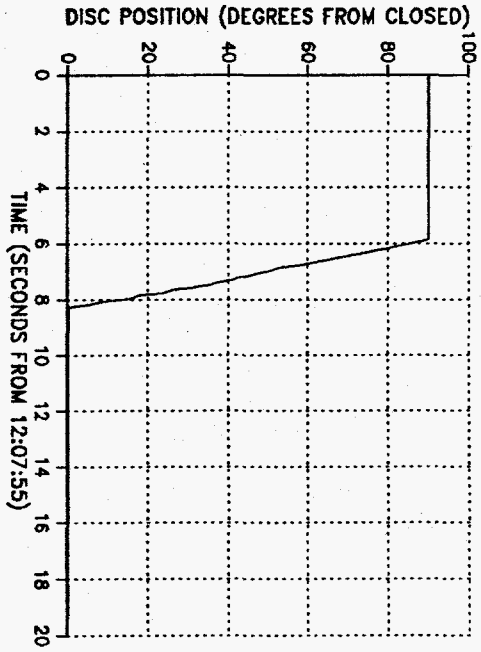
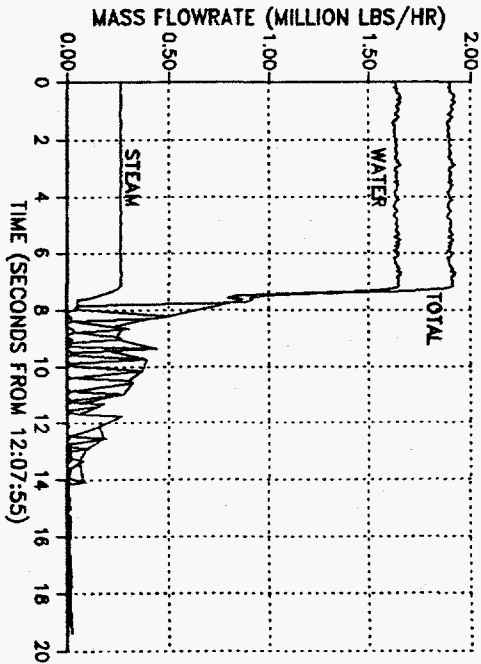


Figure 7.1-1. Valve 2 Closing Test, Dry Steam, 100% Quality (Test 8)

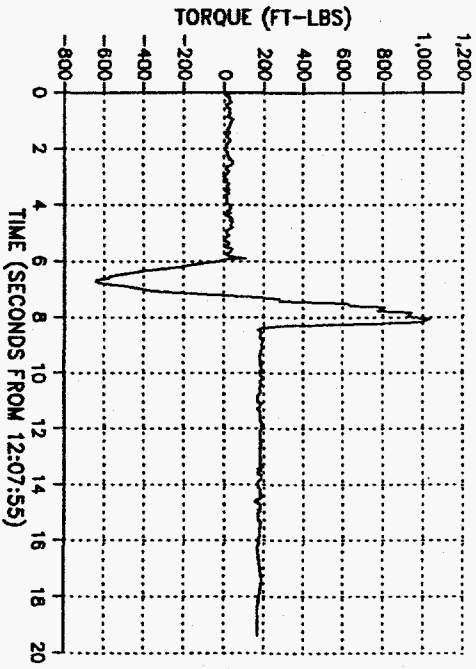
DISC POSITION



MASS FLOWRATE



VALVE TORQUE



UPSTREAM AND DOWNSTREAM PRESSURE

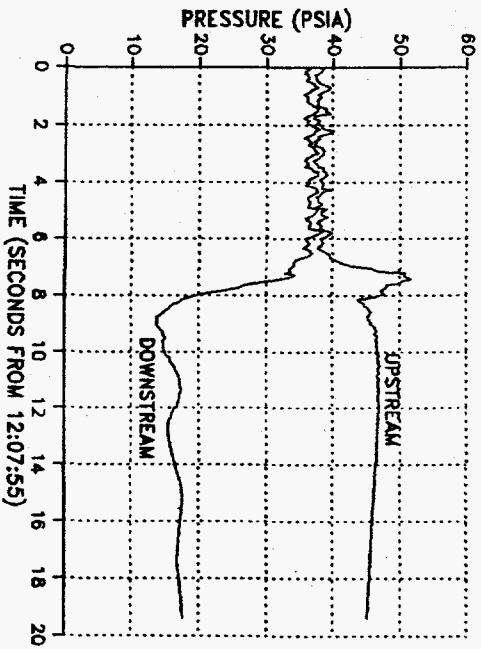


Figure 7.1-2. Valve 2 Closing Test, 28% Quality Steam (Test 13)

7.2 Full Open Disc Torque, Measured Vs. Predicted

A primary objective of the ETEC test program was to experimentally determine flow-induced torque on the butterfly valves. Prior to this full scale testing, scale model valve testing was performed and the torque values were extrapolated to the full scale valves. Section 4.3 details the method by which the valve shaft torque is linked to the steam flow parameters and the method used to extrapolate these values for the full scale valves. The scale model testing was done using only dry, saturated steam. The methodology was extended to encompass wet steam (quality = 25%) assuming the flow to be a homogeneous mixture of gas and liquid traveling at the same velocity through the valves and that the wet flow conforms to Bernoulli's equations for streamline flow. The scale model testing proved to be very conservative from the standpoint of predicting full scale flow-induced torque.

7.2.1 Dry Steam Flow

At a maximum flowrate of 3 million lbs/hr during Test 17, the measured valve torques averaged 1300 ft-lbs and 1850 ft-lbs for valves 1 and valve 2, respectively. Such a difference in torque was unexpected since both valve discs are of identical geometry. The difference indicates the importance of parameters other than flowrate and density on valve torque. In this case, the dominant variable believed to result in the torque difference is the flow pattern across each disc. The presence of the 90° elbow upstream of valve 2 certainly changes the flow pattern across valve 2 in relation to valve 1. The elbow could conceivably create a higher torque on valve 2 because of flow separation at the downstream intrados of the elbow, which is coincident with the location of the disc. Since the disc is oriented in a plane parallel to the elbow, this flow separation causes a reduced net flow area over the disc with a proportional increase in flow velocity. Since the flow-induced torque is proportional to the square of the velocity, an appreciable increase in torque is not surprising.

Figure 7.2-1 plots valve 1 and valve 2 measured torques for Test 17 against dynamic pressure, which was calculated using measured supply flowrate and density based on measured piping inlet static pressure. (Since there was no appreciable difference between pressures upstream of valve 1 and valve 2, the dynamic pressures were assumed to be equal for this figure.) For comparison, the figure also shows the predicted torque curve for the full open, full scale valve based on extrapolation of the scale model tests described in section 4.3. As seen in the figure, the measured torques are considerably less than the predicted values.

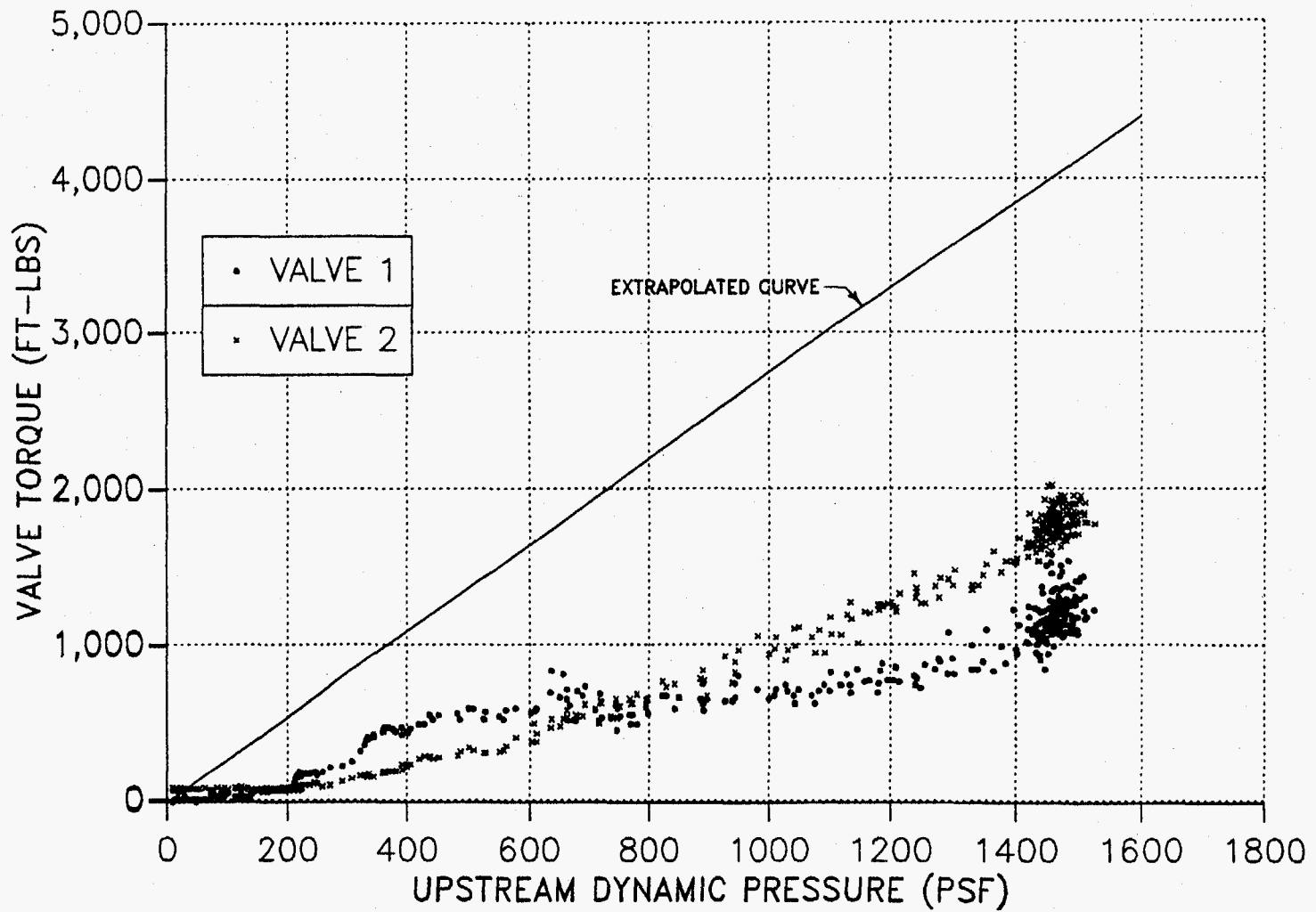


Figure 7.2-1. Comparison of Measured and Predicted Valve Flow-Induced Torques in Dry Steam (Test 17).

7.2.1 (Cont'd)

Several possible contributors to the difference in predicted versus measured flow-induced torques have been identified. These include differences in bearing friction and flow regime between the scale model tests and the LSSVT, inaccuracies in the flowrates calculated from the scale model test data, and inaccuracy in the scale factor used in extrapolating from the scale model test data.

The scale model valve disc and shaft were installed in a valve body using roller bearing shaft supports. These bearings provided very low frictional resistance to the shaft, thus allowing nearly all flow-induced torque to be transmitted through the shaft to the strain gage measuring device. The actual full scale valve used oil impregnated sleeve bushings as valve shaft supports originally, which were later replaced with Kamatics bushings (Karon B coated stainless steel) for valve 2 only. These sleeve bushings have greater frictional resistance than the roller bearings used for the scale model tests, resulting in reduced torque transmitted to the strain gage bridge measuring device.

Aside from bearing friction torque causing the measured torque to be less than the true flow-induced torque, assumptions made for analysis of the scale model test data likely resulted in a conservatively high predicted torque, further contributing to the discrepancy. As described in section 4.3.1, the scale test flowrates were determined from measured accumulator pressures, assuming that no liquid (condensate) was present in the accumulators. This assumption was necessary because no instrumentation was available to measure liquid content. By neglecting liquid content, the calculated flowrate would be less than the true flowrate for a given drop in accumulator pressure because some liquid would flash to vapor and contribute to the flow. However, the measured torque is a result of the true flowrate. Therefore, when extrapolating the measured scale model torque using the lesser calculated flowrate (and the correspondingly lower dynamic pressure), an artificially high predicted LSSVT torque would result. This effect cannot be quantified without knowing the change in liquid mass during the blowdown period.

Another contributing factor leading to the variance in measured versus predicted torque is the condition of the steam flow as it passes through the valve and across the valve disc. The scale model test piping contained several pipe diameter lengths of flow straighteners in the form of small tube bundles located upstream of the test article. These straighteners produced a steady, non-rotational flow regime. The full scale test configuration contained a flow mixer designed to inject and mix water droplets with dry steam to produce wet steam of a predetermined quality. By virtue of its intended purpose, the mixer generated a great deal of turbulence. The end result of the increased turbulence is lower flow-induced torque compared to that produced by the less turbulent flow during the scale model tests.

7.2.1 (Cont'd)

One final possible source of uncertainty in the torque extrapolation is the exponent used on the diameter ratio scale factor discussed in section 4.3.2. An exponent of 3 was used. Reference 2 notes that the exponent varies above or below 3, and is affected by disc geometry and upstream pressure. The turbulence created by the mixer described in the preceding paragraph may also affect the value of the exponent. It is not known by how much the diameter ratio scale factor exponent may differ from 3 due to the combination of different disc geometries, upstream pressures, and degree of turbulence, or in which direction it may vary. However, since the diameter ratio is only 1.74, the effect of uncertainty in the exponent is believed to be small compared to the other factors contributing to the discrepancy between predicted and measured torques.

7.2.2 Wet Steam Flow

Figure 7.2-2, presenting Test 46 results, illustrates the measured and predicted torque values for wet steam flow. This figure was developed similarly to Figure 7.2-1 for dry steam except the LSSVT torques and dynamic pressures (uniform homogeneous flow basis) are not plotted during the flow ramp-up since the quality was changing rapidly toward the intended value. Also shown is the predicted torque curve for the full open, full scale valve based on extrapolation of the scale model tests described in section 4.3. As illustrated in Figure 7.2-2, the measured LSSVT torques for wet steam flow are also considerably lower than predicted values, especially in the case of valve 1 torques.

All factors contributing to the dry steam torque discrepancy described in section 7.2.1 also apply to the wet steam flow. In addition to these factors, another factor in the over prediction of the wet steam flow-induced torque is the assumption that the wet steam behaves as a homogenous mixture—essentially a gas with a density equal to the wet steam mixture density at the specified quality. This assumption was made for simplicity, realizing that resulting torque extrapolations would provide conservative values.

Physically, the reason the homogenous flow assumption is conservative is because the liquid droplets in the flow, which make up 75% of the total mass of the flow (for 25% steam quality), are less likely to conform to streamline flow over the disc because of their inertia. A restriction of the Bernoulli equation upon which the dynamic pressure proportionality extrapolations are based is that the flow follows streamlines. Therefore, any significant sized water droplets are not believed to have contributed much to flow-induced torque. Also, impingement of water onto the disc is likely to have had a negligible effect on torque because of the relatively small projected area and symmetrical design of the disc.

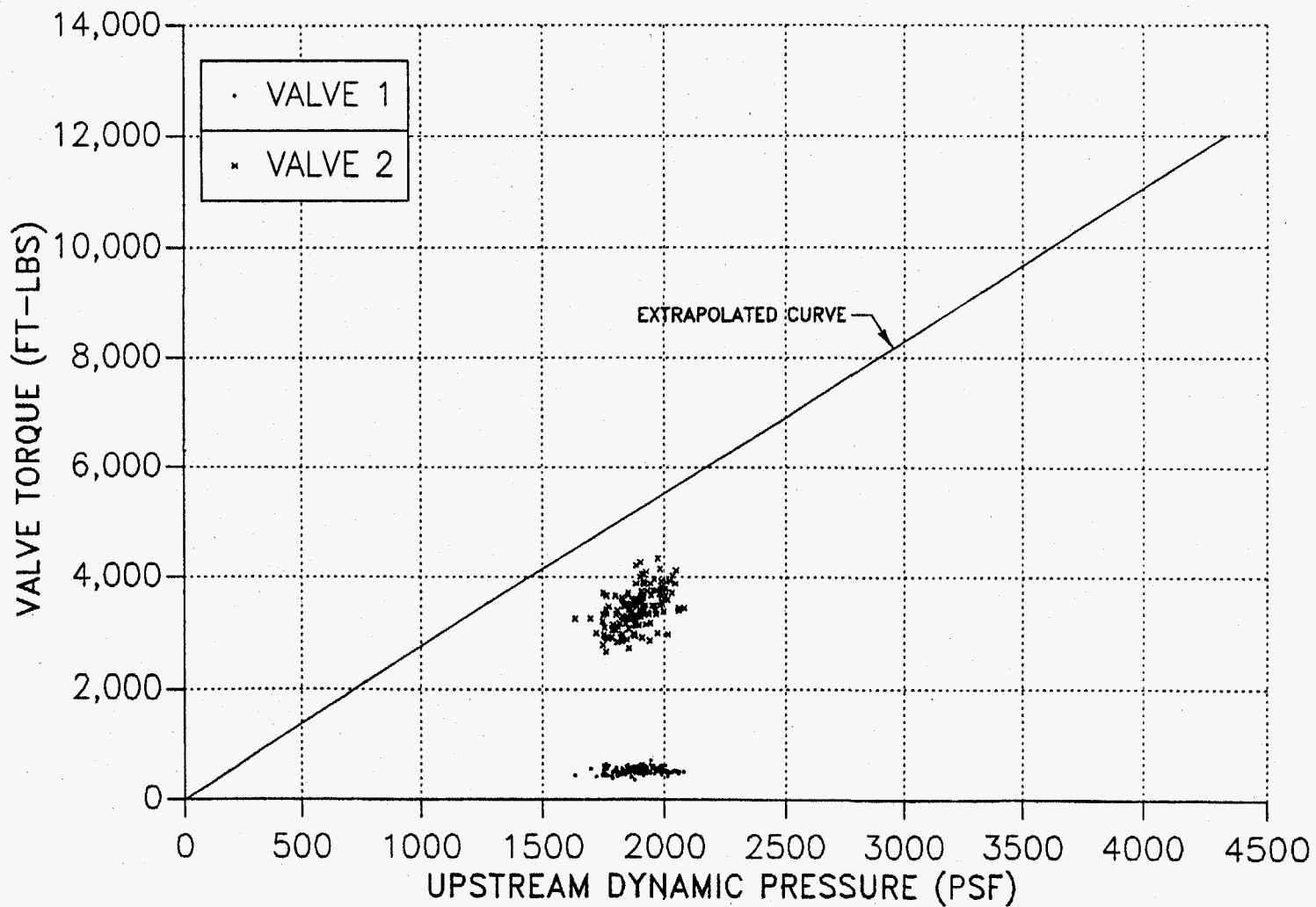


Figure 7.2-2. Comparison of Measured and Predicted Valve Flow-Induced Torques in Wet Steam (Test 46).

7.2.2 (Cont'd)

An unexpected and, as yet, not fully understood, phenomenon was observed about the valve torques during the wet steam tests. To ramp up to the intended flowrate and quality, a dry steam flow ramp was initiated first, followed by a water flow ramp about 5 seconds later. As water flow increased, steam quality dropped from 100% toward the goal of 25%. At approximately 50% quality, the two valve torques, which had been following each other closely, began to diverge. During Test 45, valve 1 torque dropped from a peak of 700 ft-lbs (while the total flowrate was only 4 million lbs/hr) to 300 ft-lbs in about 2 seconds, then varied with the total flowrate oscillations for the remainder of the test, but never exceeded 600 ft-lbs for the remainder of the test, even during the peak flow of 9.75 million lbs/hr.

The torque response of valve 2 was even more unusual. After the 2 seconds during which the valve 1 torque dropped from 700 to 300 ft-lbs, the valve 2 torque jumped from 900 ft-lbs to 3000 ft-lbs over the next 1.5 seconds. During the rest of the test, the valve 2 torque oscillated as much as 2000 ft-lbs—sometimes out of phase with the flowrate oscillations—reaching a peak torque of 4700 ft-lbs with a flowrate of 7.4 million lbs/hr. As the flowrate continued to increase toward the peak, the valve 2 torque oscillations decreased toward an average of about 3000 ft-lbs.

Figure 7.2-3 shows a plot of the valve torques during Test 45, illustrating the torque divergence. Also shown in the figure for comparison are plots of related parameters—steam, water, and total supply flowrates; inlet steam quality; and piping static pressures upstream of each valve over the same time interval.

The divergence between the two measured valve torques seen in Test 45 occurred in all the wet steam tests with some variations. For comparison, Figure 7.2-4 presents similar data for Test 46. During the flow ramp-up, both valve torques followed each other closely up to about 1200 ft-lbs before they diverged (compared to 700 ft-lbs for Test 45). Again, this divergence occurred when the quality dropped below 50%, although this quality is not believed to be a threshold above which the divergence will not occur because the divergence also occurred in Test 50 with 75% quality. Three seconds later, valve 1 torque reached a minimum of about 300 ft-lbs, then steadily increased to 700 ft-lbs as flowrate increased. About 1 second after valve 1 reached its minimum, the valve 2 torque began its jump from 1200 ft-lbs to 3000 ft-lbs in only 1.5 seconds, then increased in smaller scale oscillations than for Test 45, to a peak of 4300 ft-lbs and averaged about 3700 ft-lbs.

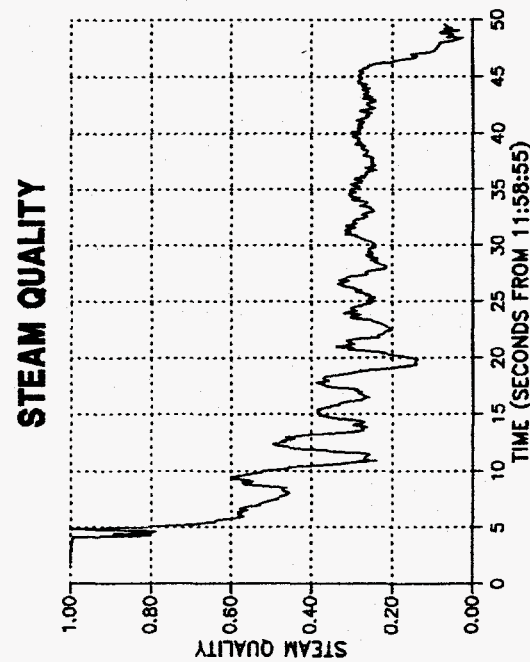
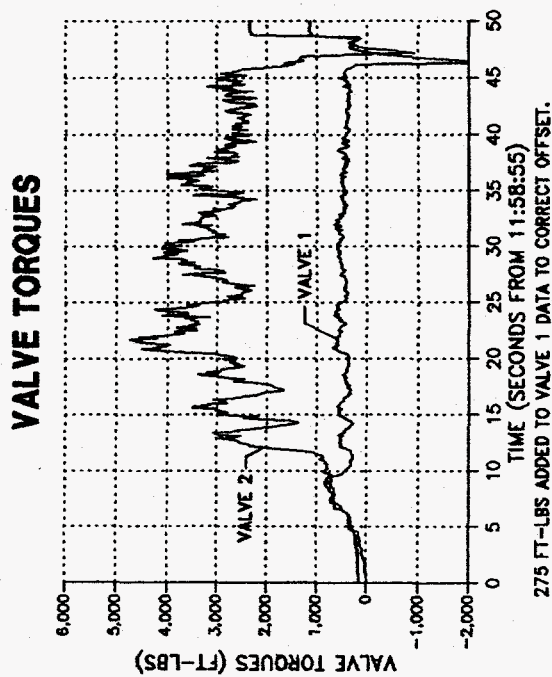
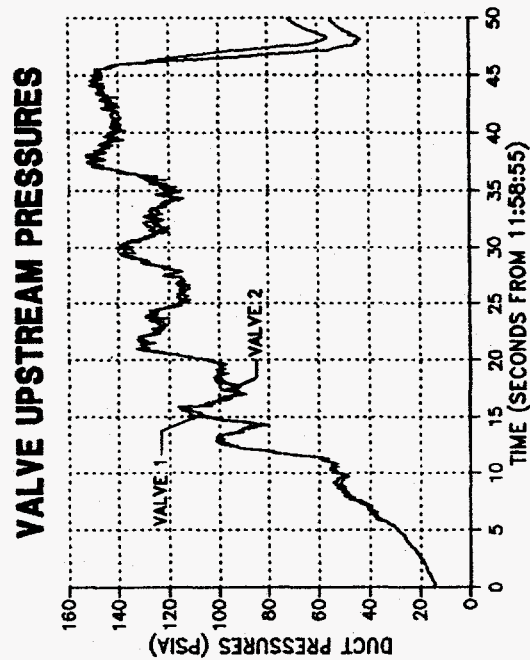
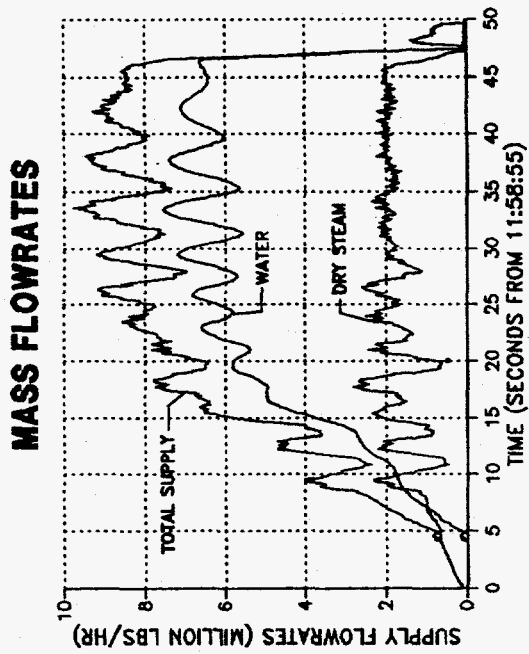
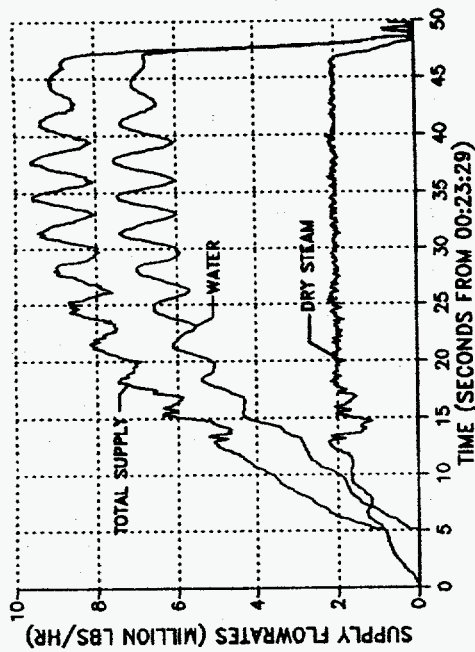
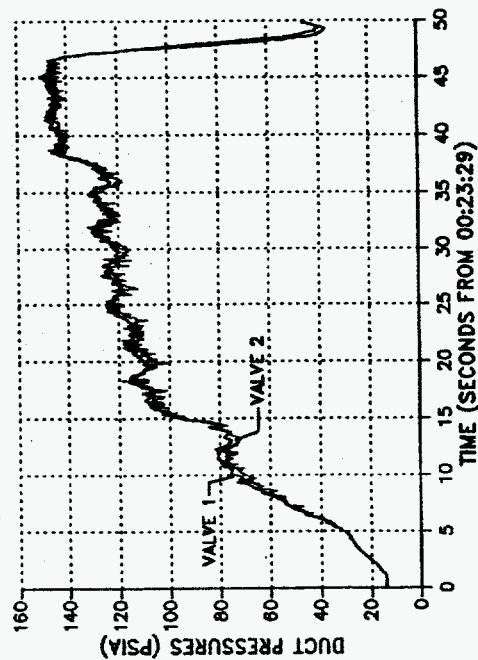


Figure 7.2-3. Comparison of Valve Torques to Related Parameters (Test 45).

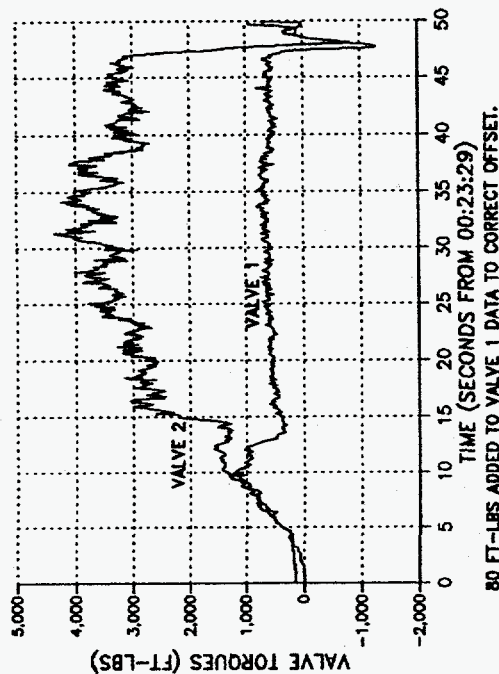
MASS FLOWRATES



VALVE UPSTREAM PRESSURES



VALVE TORQUES



80 FT-LBS ADDED TO VALVE 1 DATA TO CORRECT OFFSET.

STEAM QUALITY

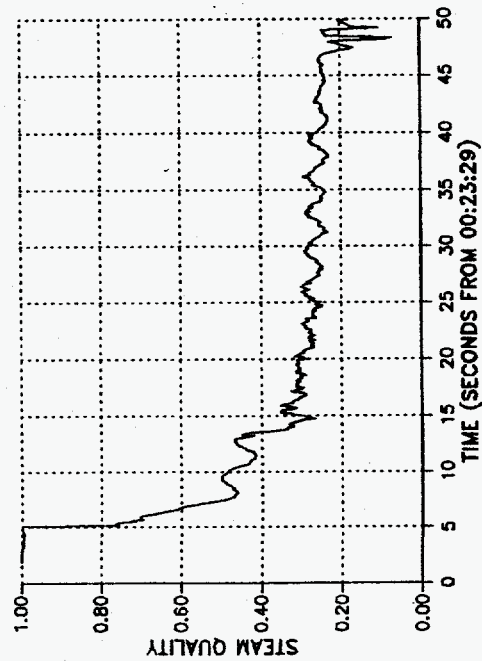


Figure 7.2-4. Comparison of Valve Torques to Related Parameters (Test 46).

7.2.2 (Cont'd)

Obviously, the presence of entrained liquid somehow affected the torque measurements. Several theories are proposed to explain what effects the liquid may have had. The first theory explaining the rise in valve 2 torque expands on the previously noted effect of flow separation at the elbow possibly causing the slightly higher torques for valve 2 during dry steam flow. If the liquid creates greater separation and therefore reduced net flow area and higher flow velocity in the vicinity of the valve 2 disc, higher torque would result. A mechanism by which the liquid may cause greater separation is explained by considering the trajectory the liquid droplets would be expected to take through the elbow upstream of valve 2. Because of the droplets' inertia, they would tend to be flung toward the outer wall of the elbow at some angle to the vapor flow streamlines. Viscous forces between the droplets and vapor would tend to "drag" the vapor more toward the outer elbow wall, causing a larger separation zone, reduced net flow area, and higher flow velocity over the valve 2 disc, and thus, higher torque.

The liquid may have also affected the torque as a result of direct liquid impingement on the disc. As mentioned above, water impingement is not considered to have had a significant direct effect on torque because of the relatively small projected area and symmetrical design of the disc. However, for valve 2, it may be more significant because of the liquid being de-entrained onto the outer elbow wall, which would cause a possible heavy concentration of liquid impinging against the disc in the vicinity of the actuator drive shaft pillow block. But because of the small lever arm with which this impingement force could generate torque, the effect of this type of impingement is still considered to be small.

A secondary effect of liquid impingement on valve 2 torque, aside from flow-induced torque, may be that the impingement force reduces the resultant shaft bearing reaction force, thereby reducing friction torque (see section 7.2.1), allowing more torque to be transmitted through the bearing to the strain gage for measurement. The valve 2 shafts are oriented horizontally so that the weight of the disc (650 lbs) loads the bearings at no flow. Because of the orientation of the valve relative to the upstream elbow, the liquid on the outer wall of the elbow impinges on the disc and exposed shaft in an upward direction, tending to oppose the downward force due to the disc weight and actuator force. In this way, bearing friction is reduced, allowing more flow-induced torque to be transmitted to the strain gage.

The liquid impingement on the valve 2 disc may also increase flow-induced vibration on the disc, which as described in section 7.2.1, is believed to cause dissipation of at least part of the friction torque resulting in greater measured torque.

The above described theories offer explanations for the marked increase in valve 2 torque, but do not address the drop in valve 1 torque despite increasing flow. The fact that the sudden change in the torque of each valve occurs nearly simultaneously indicates that they share a common cause—presumably entrained liquid since the changes occur during the addition of liquid to the flow.

7.2.2 (Cont'd)

One explanation of the drop in valve 1 torque considered the effect of a larger separation zone at valve 2, theorized to be caused by the liquid. If this occurred causing a restriction to flow, higher velocity, and greater pressure drop through valve 2, the resulting rise in pressure at valve 1 would tend to reduce its torque. However, static pressures recorded upstream and downstream of valve 2 do not clearly show an increase in pressure drop across valve 2 significant enough to account for the measured drop in valve 1 torque. It should be noted, however, that at the time of interest, the liquid and steam flowrates were ramping up in an oscillatory manner, and the piping pressures and valve torques had measurement fluctuations superimposed on the real values that makes it difficult to determine causal relationships between these measurements. Therefore, the possibility that increased separation at valve 2 also causes the decrease in valve 1 torque cannot be entirely dismissed, but it does seem unlikely.

Liquid may have a more direct effect on decreasing valve 1 torque that is independent of any effect it has on valve 2 torque. Since valve 1 is located just a few feet downstream of the mixer, it is presumed that liquid is fairly evenly distributed across the flow area, as opposed to valve 2 where the elbow will cause much liquid to be de-entrained against the outer wall. As a result, some liquid droplets would strike the leading edge, and upper and lower surfaces of the valve 1 disc. The effect of the droplet impacts is theorized to increase the turbulence in the boundary layer, which tends to delay the point of flow separation on the downstream half of the disc. By reducing the disc area over which separation exists, the difference in pressure distribution between the front and rear halves of the disc, and therefore, flow-induced torque, is reduced.

8. Summary and Conclusions

This section summarizes the main conclusions and significant findings resulting from the LSSVT program and follow-up analyses.

Flow-Induced Torque Reduction

One of the primary objectives of the butterfly valve redesign was to reduce the torque generated by flow on the valve disc. The LSSVT and prior scale model disc testing verified that the new thinner, more symmetrically shaped disc offered a significant reduction in torque over the old design for the same flow conditions. This verification, together with other elements of the redesign which upgraded the capabilities of other valve components, results in significant margin in the ability of the valves to withstand high flowrate conditions.

The maximum dry steam flow condition was shown to generate greater valve 1 torque than the maximum wet (25% quality) flow condition, despite the fact that the wet steam mass flowrate was more than a factor of three greater than that of the dry steam. This result was attributed to the belief that entrained liquid did not contribute significantly to the torque, and may have possibly reduced the ability of the vapor phase to generate torque by altering the vapor flow pattern over the disc. One exception to this conclusion is the finding that for valve 2, which is located immediately downstream of a 90° elbow, the apparent combined effects of the elbow and entrained liquid resulted in a marked increase in measured flow-induced torque over valve 1 torque during the same test.

Valve Operation

The ability of the butterfly valves to function as required under high flowrate conditions was successfully demonstrated. No problems were encountered when demonstrating the ability of the valve to close against required flowrates without sustaining damage.

Valve Flow-Induced Torque Divergence in Wet Steam Flow

An unexpected and not fully understood phenomenon was observed about the valve torques in wet steam flow. During the flow ramp-up for each wet steam test, the valve 1 torque decreased despite increasing flow, and the valve 2 torque almost simultaneously increased to a level an order of magnitude greater than valve 1. Several mechanisms are theorized by which the combined effects of the entrained liquid and the 90° elbow upstream of valve 2 could result in the observed torques. These include mechanisms that directly or indirectly affect the flow-induced torque as well as means by which the liquid could decrease valve 2 bearing friction, allowing more torque to be transmitted through the bearing where it can be measured. No firm conclusions could be drawn regarding the causes of the torque divergence.

9. References

1. Silvester, R. S. April 1980. "Torque Induced By Compressible Flow Through a Butterfly Valve with an Asymmetric Disc Design." BHRA Fluid Engineering. (RR-1602)
2. Watkins, John C. et al. August 1986. "A Study of Typical Nuclear Containment Purge Valves in an Accident Environment." NUREG/CR-4648, EGG-2459, EG&G Idaho, Inc.
3. Steele, Robert and John C. Watkins. September 1985. "Containment Purge and Vent Valve Test Program Final Report." NUREG/CR-4141, EGG-2374, EG&G Idaho, Inc.

100